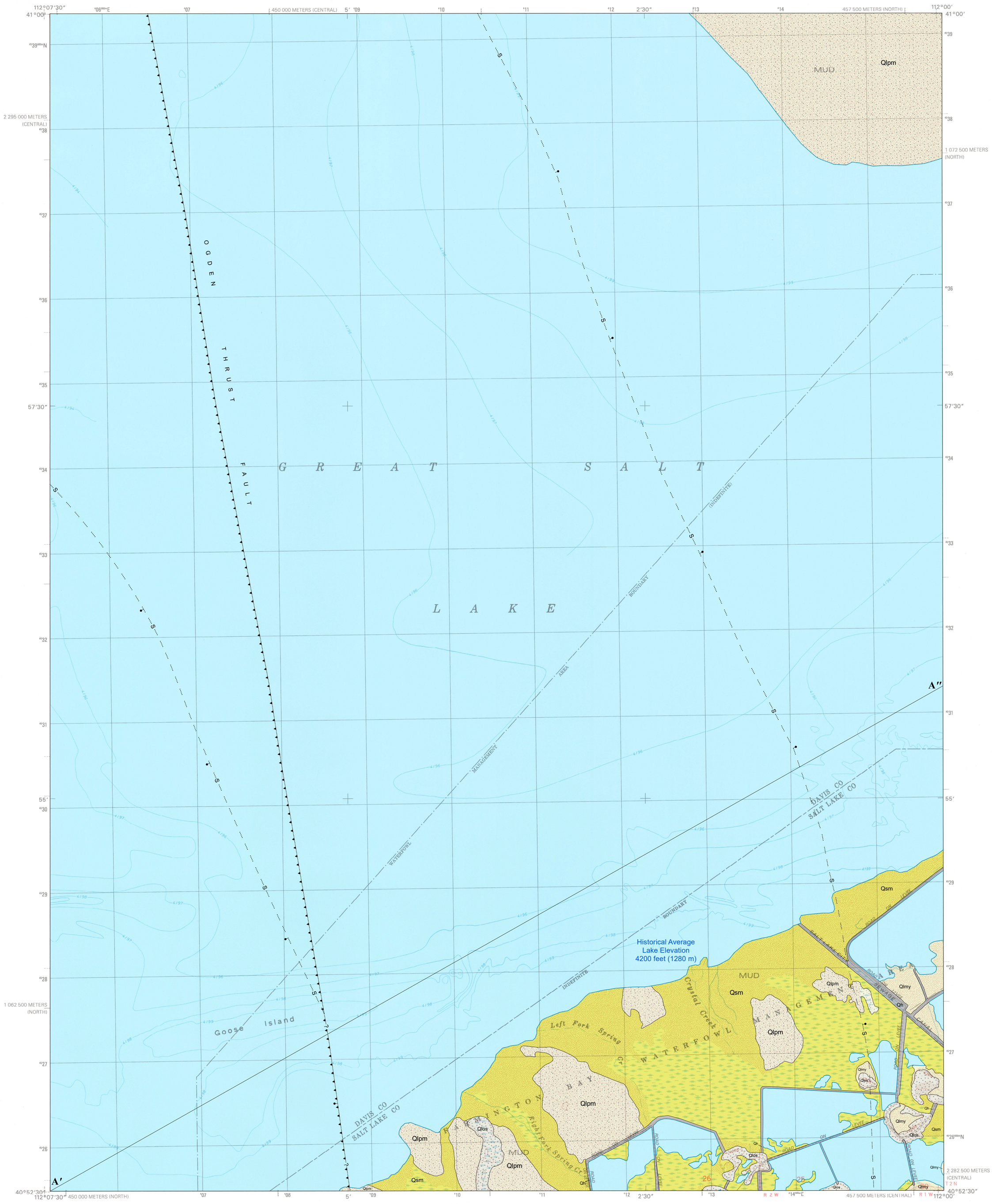
UTAH GEOLOGICAL SURVEY
a division of
Utah Department of Natural Resources

Plate 1
Utah Geological Survey Map 282DM
Geologic Map of the Saltair NE Quadrangle



SCALE 1:24,000

1 0.5 0 1 MILE

1000 0 1000 2000 3000 4000 5000 6000 7000 FEET

1 0.5 0 1 KILOMETER

CONTOUR INTERVAL 5 FEET
BATHYMETRIC CONTOUR INTERVAL 1 FOOT

11°22′
TRUE NORTH
MAGNETIC NORTH
APPROXIMATE MEAN DECLINATION, 2019

GEOLOGIC MAP OF THE SALTAIR NE QUADRANGLE, SALT LAKE AND DAVIS COUNTIES, UTAH

by

Adam P. McKean

2019

Although this product represents the work of professional scientists, the Utah Department of Natural Resources, Utah Geological Survey, makes no warranty, expressed or implied, regarding its suitability for a particular use, and does not guarantee accuracy or completeness of the data. The Utah Department of Natural Resources, Utah Geological Survey, shall not be liable under any circumstances for any direct, indirect, special, incidental, or consequential damages with respect to claims by users of this product. Geology intended for use at 1:24,000 scale.

This map was created from geographic information system (GIS) files. It meets formal Utah Geological Survey GIS and cartographic standards for publication. Persons or agencies using these data specifically agree not to misrepresent the data, nor to imply that changes they made were approved by the Utah Geological Survey, and should indicate the data source and any modifications they make on plots, digital copies, derivative products, and in metadata.



QUADRANGLE LOCATION

Base from USGS Saltair NE 7.5′ Quadrangle (1997)
Projection: UTM Zone 12
Datum: NAD 1983

Project Manager: Donald L. Clark
Aerial photo and field mapping of geology:
Adam P. McKean, 2012-2013
GIS and Cartography: Adam P. McKean and Martha L. Jensen

Utah Geological Survey
1594 West North Temple, Suite 3110
Salt Lake City, UT 84116
(801) 537-3300
geology.utah.gov

1	2	3
4	·	5
6	7	8

1. Antelope Island North
2. Clearfield
3. Kaysville
4. Antelope Island
5. Farmington
6. Antelope Island South
7. Baileys Lake
8. Salt Lake City North

ADJOINING 7.5′ QUADRANGLE NAMES

UTAH GEOLOGICAL SURVEY
a division of
Utah Department of Natural Resources

Plate 2
Utah Geological Survey Map 280DM, 281DM, and 283DM
Geologic Maps of the Antelope Island South, Baileys Lake, and Saltair NE 7.5' Quadrangles

GEOLOGIC SYMBOLS

- Contact – Dashed where approximately located; dotted where concealed
- Normal fault – Dashed where approximately located, dotted where concealed; bar and ball on downthrown side; arrow shows dip of the fault; arrows on cross section indicate direction of relative movement
- Normal fault, geophysical, seismic – Located from shallow seismic reflection data for Great Salt Lake fault zone (from Clark and others, 2017); heavier line for main faults and lighter line for subsidiary faults; dashed where approximately located; dotted where concealed; bar and ball on downthrown side; colors indicate relative age of youngest sediments affected by faulting:
  - Main fault (red) with lake bottom displacement
  - Subsidiary fault (green) with Holocene sediments affected
  - Subsidiary fault (blue) with pre-Holocene sediments affected
- Unconfirmed normal fault – Trace modified from Janecke and Evans (2017); bar and ball on downthrown side
- Normal fault, geophysical, seismic – Located from seismic data, concealed and very approximately located; bar and ball on downthrown side
- Normal fault, geophysical, gravity – Located from gravity data, concealed and very approximately located; bar and ball on downthrown side
- Thrust fault – Dotted where concealed; dotted and queried where existence and location inferred; teeth on hanging wall; bar and ball where reactivated as normal fault
- Inferred transverse fault zone – Dotted and queried where concealed and very approximately located
- Shear zone in metamorphic bedrock, trend approximates dominant shear direction
- Quartz vein in metamorphic bedrock
- Pit extent, aggregate sand and gravel operations
- A—A″ Line of cross section

- Lacustrine shorelines – Major shorelines of the Bonneville lake cycle, Gilbert-episode lake, and Great Salt Lake. Mapped at the upper nick point of wave-cut bench for erosional shorelines and the top of constructional bars and barrier beaches; may coincide with geologic contacts; dashed where approximately located:
  - S — Lake Bonneville, Stansbury shoreline
  - B — Lake Bonneville, Bonneville shoreline
  - P — Lake Bonneville, Provo shoreline
  - G — Gilbert-episode shoreline
  - I — Great Salt Lake, Holocene intermediate shoreline
  - H — Great Salt Lake, late Holocene highstand shoreline
  - h — Great Salt Lake, historical highstand shoreline
- Crest of lacustrine barrier bar or spit
- Natural levee deposits, may coincide with Great Salt Lake shorelines (units Qdy, Qdd)
- Structural and metamorphic measurements – from Doelling and others (1990, 2018)
  - 15 — Strike and dip of cleavage
  - Vertical cleavage
  - 30 — Strike and dip of metamorphic foliation
  - Vertical foliation
- Spring
- Sand and gravel pit
- Water well (selected)
- DH1 — Oil and gas exploration well, plugged and abandoned (see table 3)
- SC1 — Sediment core (selected, see table 5)
- RC1 — Geochronology sample (McKean and others, 2016; see table 2)
- ZR1 — U-Pb zircon geochronology sample (Nelson and others, 2011; see table 6)
- Paleoseismic trench (Hylland and others, 2014)
- Qsm/Qaly — Stacked unit – Denotes thin cover of first unit overlying second unit

MAP UNITS
(see booklet for complete unit descriptions)

ANTELOPE ISLAND SOUTH

- Qal$_s$ Modern stream deposits
- Qafy Younger alluvial-fan deposits
- Qdy Younger deltaic deposits
- Qh Fill and disturbed land
- Qht Tailings
- Qlb Lacustrine boulders
- Qlg Lacustrine gravel and sand
- Qlgy Young lacustrine gravel and sand
- Qlgb Lacustrine gravel and sand related to Bonneville shoreline and transgressive phase of Lake Bonneville
- Qll Lagoon-fill deposits
- Qlos Lacustrine oolitic sand deposits
- Qlpn Lacustrine and playa mud deposits
- Qlmy Young lacustrine mud deposits
- Qlmk Lacustrine mud and microbial carbonates
- Qsm Spring and marsh deposits
- Qldy Young lacustrine and deltaic deposits
- Qh/Tsl Human disturbance over Salt Lake Formation, undivided
- Xfc Farmington Canyon Complex, undivided (see cross section)
- KXa Farmington Canyon Complex, altered and deformed rocks
- Xfcp Farmington Canyon Complex, granite and pegmatite
- Xfcb Farmington Canyon Complex, banded gneiss
- Xfcu Farmington Canyon Complex, metamorphosed ultramafic rock
- Xfcq Farmington Canyon Complex, quartz-rich gneiss
- Xfcl Farmington Canyon Complex, layered gneiss

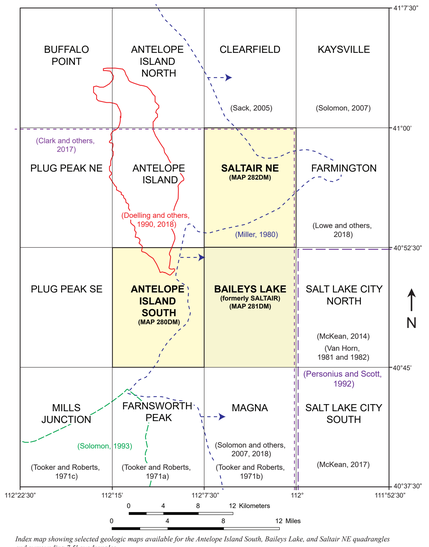
BAILEYS LAKE

- Qal$_s$ Modern stream deposits
- Qaly Young stream deposits, undivided
- Qalg Stream deposits related to Gilbert-episode lake and/or Great Salt Lake
- Qat Stream terrace deposits
- Qdy Younger deltaic deposits
- Qdd Deltaic distributary channel-fill deposits
- Qdf Deltaic-fan deposits
- Qdg Deltaic deposits related to Gilbert-episode lake and/or Great Salt Lake
- Qh Fill and disturbed land
- Qht Tailings
- Qlos Lacustrine oolitic sand deposits
- Qlpm Lacustrine and playa mud deposits
- Qlmy Young lacustrine mud deposits
- Qly Young lacustrine deposits
- Qsm Spring and marsh deposits
- Qldy Young lacustrine and deltaic deposits
- Qsm/Qaly Spring and marsh deposits over young stream deposits, undivided

SALTAIR NE

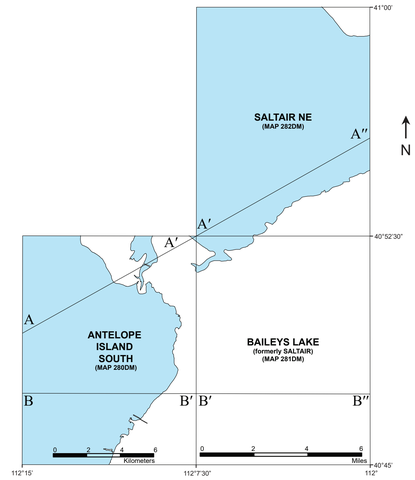
- Qh Fill and disturbed land
- Qlos Lacustrine oolitic sand deposits
- Qlpm Lacustrine and playa mud deposits
- Qlmy Young lacustrine mud deposits
- Qsm Spring and marsh deposits

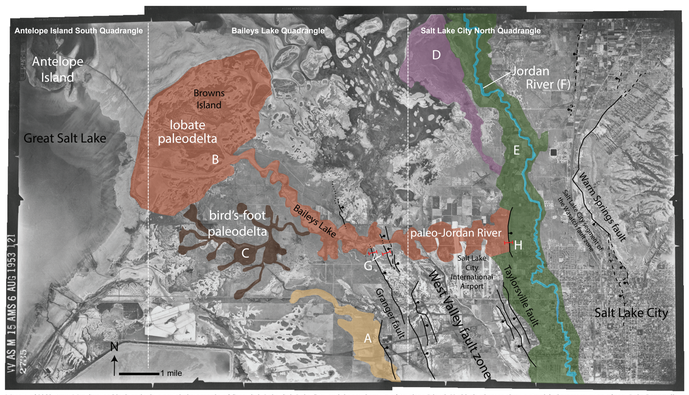
INDEX TO GEOLOGIC MAPPING



Index map showing selected geologic maps available for the Antelope Island South, Baileys Lake, and Saltair NE quadrangles and surrounding 7.5' quadrangles.

INDEX TO CROSS SECTIONS A-A″ AND B-B″





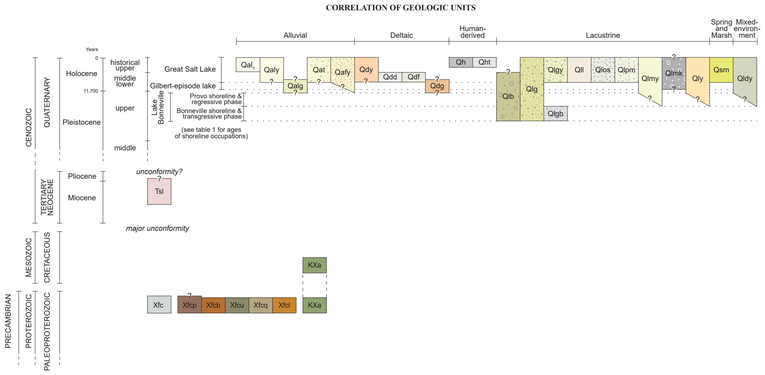
Mosaic of 1953 Army Map Service black-and-white aerial photographs of Great Salt Lake, Salt Lake City, and the southern tip of Antelope Island. Highlighted areas show a simplified representation of post-Lake Bonneville river channels and deltaic deposits. (A) Gilbert-episode river channel and paleodelta deposited as the lake receded. (B) post-Gilbert, west-flowing paleo-Jordan River and associated lobate paleodelta. (C) bird's-foot paleodelta that was likely deposited during the late Holocene highstand of Great Salt Lake. (D) paleodelta deposited during northward flow of the Jordan River. (E) approximate location of Jordan River meander floodplain. (F) modern modified channel of the Jordan River. (G) location of 2010 paleoseismic trenches on the Granger fault (Hylland and others, 2014). (H) location of 1997 and 2015 paleoseismic trenches on the Taylorsville fault (Solomon, 1998; Hylland and others, 2017). Simplified fault zones shown for reference only, location and orientation approximate, see geologic maps for mapped locations.

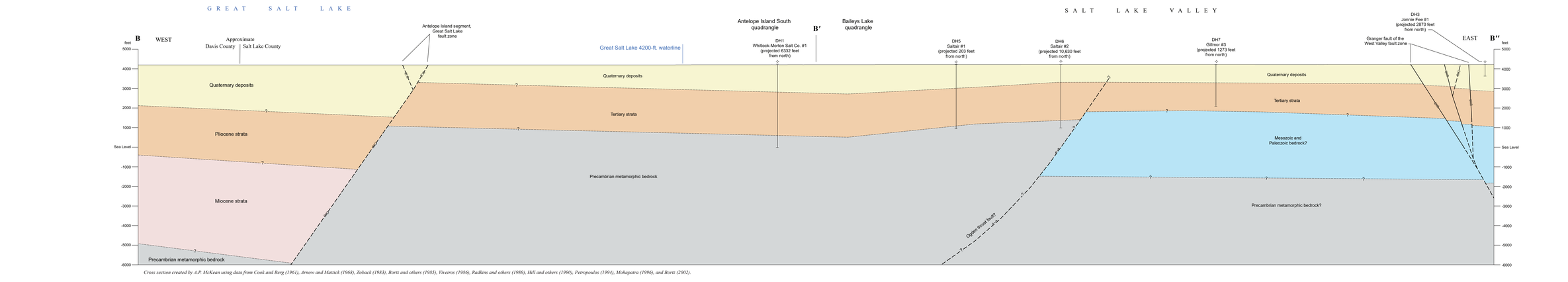
LITHOLOGIC COLUMN

AGE	Geologic Unit	MAP UNIT SYMBOL	THICKNESS Feet (Meters)	LITHOLOGY
TERTIARY NEOGENE: PLIO.? / MIOCENE	Salt Lake Formation	Tsl	1800+ feet (550+ m)	6.1 ± 1.1 Ma Zr fission track (Bryant and others, 1989); 8–11 Ma tephrochronology (Willis and Jensen, 2000)
PALEOPROTEROZOIC	Farmington Canyon Complex: Altered and deformed rocks	KXa	variable	Major unconformity; Altered and deformed in Cretaceous (KXa) (Yonkee, 1990)
	Granite and pegmatite	Xfcp		
	Banded gneiss	Xfcb		1691 ± 26 Ma U-Pb zircon (Xfcl) (sample 01FCC6, Nelson and others, 2011)
	Metamorphosed ultramafic rock	Xfcu		1640 to 1720 Ma $^{207}Pb/^{206}Pb$ - monazite from gneisses (Barnett and others, 1993)
	Quartz-rich gneiss	Xfcq		
	Layered gneiss	Xfcl		1705 ± 90 Ma mean monzonite microprobe age from a gneiss (Nelson and others, 2002, 2011)

Modified from Doelling and others (1990, 2018), Yonkee and others (2000a), and Clark and others (2017)
*Some Farmington Canyon Complex units shown are not in the study area

CORRELATION OF GEOLOGIC UNITS





Cross section created by A.P. McKean using data from Cook and Berg (1961), Zoback (1983), Bortz and others (1985), Viveiros (1986), Wilson and others (1986), Lambert and West (1989), McNeil and Smith (1992), Yonkee (1992), Petropoulos (1994), Mohapatra (1996), Willis and Jensen (2000), Bortz (2002), and Willis and others (2010).

Cross section created by A.P. McKean using data from Cook and Berg (1961), Arnow and Mattick (1968), Zoback (1983), Bortz and others (1985), Viveiros (1986), Radkins and others (1989), Hill and others (1990), Petropoulos (1994), Mohapatra (1996), and Bortz (2002).

Booklet to accompany three geologic maps:

GEOLOGIC MAP OF THE ANTELOPE ISLAND SOUTH QUADRANGLE, SALT LAKE, DAVIS, AND TOOELE COUNTIES, UTAH

Utah Geological Survey Map 280DM

by Adam P. McKean, Hellmut H. Doelling, Grant C. Willis, and W. Adolph Yonkee

GEOLOGIC MAP OF THE BAILEYS LAKE QUADRANGLE, SALT LAKE AND DAVIS COUNTIES, UTAH

Utah Geological Survey Map 281DM

by Adam P. McKean and Michael D. Hylland

GEOLOGIC MAP OF THE SALTAIR NE QUADRANGLE, SALT LAKE AND DAVIS COUNTIES, UTAH

Utah Geological Survey Map 282DM

by Adam P. McKean



ACCOMPANIES MAPS 280DM, 281DM, AND 282DM
UTAH GEOLOGICAL SURVEY
a division of
Utah Department of Natural Resources
2019

Blank pages are intentional for printing purposes

Booklet to accompany three geologic maps:

GEOLOGIC MAP OF THE ANTELOPE ISLAND SOUTH QUADRANGLE, SALT LAKE, DAVIS, AND TOOELE COUNTIES, UTAH

Utah Geological Survey Map 280DM

by Adam P. McKean[1], Hellmut H. Doelling[2], Grant C. Willis[1], and W. Adolph Yonkee[3]

[1]Utah Geological Survey, P.O. Box 146100, Salt Lake City, UT 84114–6100
[2]Utah Geological Survey, retired
[3]Department of Geosciences, Weber State University, Ogden, UT 84408

GEOLOGIC MAP OF THE BAILEYS LAKE QUADRANGLE, SALT LAKE AND DAVIS COUNTIES, UTAH

Utah Geological Survey Map 281DM

by Adam P. McKean and Michael D. Hylland

GEOLOGIC MAP OF THE SALTAIR NE QUADRANGLE, SALT LAKE AND DAVIS COUNTIES, UTAH

Utah Geological Survey Map 282DM

by Adam P. McKean

SCALE: 1:24,000

Cover photo: *View to the north of Great Salt Lake southeastern shore and Antelope Island in the distance. The bedrock on southern Antelope Island is composed of Paleoproterzoic Farmington Canyon Complex.*

ACCOMPANIES MAPS 280DM, 281DM, AND 282DM
UTAH GEOLOGICAL SURVEY
a division of
Utah Department of Natural Resources
2019

STATE OF UTAH
Gary R. Herbert, Governor

DEPARTMENT OF NATURAL RESOURCES
Michael Styler, Executive Director

UTAH GEOLOGICAL SURVEY
R. William Keach II, Director

PUBLICATIONS
contact
Natural Resources Map & Bookstore
1594 W. North Temple
Salt Lake City, UT 84116
telephone: 801-537-3320
toll-free: 1-888-UTAH MAP
website: mapstore.utah.gov
email: geostore@utah.gov

UTAH GEOLOGICAL SURVEY
contact
1594 W. North Temple, Suite 3110
Salt Lake City, UT 84116
telephone: 801-537-3300
website: geology.utah.gov

Although this product represents the work of professional scientists, the Utah Department of Natural Resources, Utah Geological Survey, makes no warranty, expressed or implied, regarding its suitability for a particular use, and does not guarantee accuracy or completeness of the data. The Utah Department of Natural Resources, Utah Geological Survey, shall not be liable under any circumstances for any direct, indirect, special, incidental, or consequential damages with respect to claims by users of this product. Geology intended for use at 1:24,000 scale.

The geologic map of the Baileys Lake quadrangle was funded by the Utah Geological Survey and the U.S. Geological Survey, National Cooperative Geologic Mapping Program, through USGS STATEMAP award number G12AC20226 (2012). The views and conclusions contained in this document are those of the authors and should not be interpreted as necessarily representing the official policies, either expressed or implied, of the U.S. Government.

The geologic maps of the Antelope Island South and Saltair NE quadrangles were funded by the Utah Geological Survey.

These maps were created from geographic information system (GIS) files. Persons or agencies using these data specifically agree not to misrepresent the data, nor to imply that changes they made were approved by the Utah Geological Survey, and should indicate the data source and any modifications they make on plots, digital copies, derivative products, and in metadata. They meet formal Utah Geological Survey GIS and cartographic standards for publication.

Suggested bibliographic citations for the geologic maps this booklet accompanies:

McKean, A.P., Doelling, H.H., Willis, G.C., and Yonkee, W.A., 2019, Geologic map of the Antelope Island South quadrangle, Salt Lake, Davis, and Tooele Counties, Utah: Utah Geological Survey Map 280DM, 28 p., 2 plates, scale 1:24,000.

McKean, A.P., and Hylland, M.D., 2019, Geologic map of the Baileys Lake quadrangle, Salt Lake and Davis Counties, Utah: Utah Geological Survey Map 281DM, 28 p., 2 plates, scale 1:24,000.

McKean, A.P., 2019, Geologic map of the Saltair NE quadrangle, Salt Lake and Davis Counties, Utah: Utah Geological Survey Map 282DM, 28 p., 2 plates, scale 1:24,000.

CONTENTS

INTRODUCTION 1
PREVIOUS WORK 1
GEOLOGIC SUMMARY 1
Bedrock Stratigraphy and Geologic Structure 2
Surficial Geology 2
Ooids 4
Drill Hole Data 4
Saltair #1 (DH5) 4
Saltair #2 (DH6) 4
Whitlock-Morton Salt Co. #1 (DH1) 6
Other wells 6
Sediment cores 6
Seismic Data 6
Baileys Lake 6
Farmington Bay of Great Salt Lake 10
South arm of Great Salt Lake 10
METHODS 10
SELECTED GEOLOGIC HAZARDS 11
Surface-Fault Rupture 11
West Valley fault zone, Granger fault 11
Great Salt Lake fault zone, Antelope Island segment 12
Lake Flooding 13
SUMMARY OF HYDROGEOLOGY 13
MAP UNIT DESCRIPTIONS 13
QUATERNARY 13
Alluvial Deposits 13
Deltaic Deposits 15
Human-Derived 16
Lacustrine Deposits 16
Spring and Marsh Deposits 20
Mixed-Environment Deposits 20
Stacked-Unit Deposits 20
TERTIARY (NEOGENE) 21
CRETACEOUS TO PALEOPROTEROZOIC 21
ACKNOWLEDGMENTS 23
REFERENCES 23

FIGURES

Figure 1. Schematic northwest-southeast cross section of surficial geology 5
Figure 2. Landsat 5 “natural color” image of the 1987 Great Salt Lake flooding 14
Figure 3. Ooid sample trench 18
Figure 4. Bonneville and post-Bonneville deposits exposed in the canal cut of the Goggin Drain 19
Figure 5. Desiccated and eroded carbonate microbialite mounds on southeastern shore of Great Salt Lake 20

TABLES

Table 1. Ages of major shoreline occupations of Lake Bonneville, Gilbert-episode lake, and Great Salt Lake and shoreline elevations in the Baileys Lake, Antelope Island South, and Saltair NE quadrangles 3
Table 2. Summary of radiocarbon age analyses from the Antelope Island South quadrangle 6
Table 3. Summary of oil and gas exploration drill holes/wells from the Baileys Lake and Antelope Island South quadrangles and other quadrangles near the map area 7
Table 4. Summary of selected water wells from near the mapped area 8
Table 5. Summary of sediment cores and tephrochronology data from the Baileys Lake quadrangle 9
Table 6. Summary of SHRIMP U-Pb zircon age analysis from the Antelope Island South quadrangle 22

GEOLOGIC MAP OF THE ANTELOPE ISLAND SOUTH QUADRANGLE, SALT LAKE, DAVIS, AND TOOELE COUNTIES, UTAH

by Adam P. McKean, Hellmut H. Doelling, Grant C. Willis, and W. Adolph Yonkee

GEOLOGIC MAP OF THE BAILEYS LAKE QUADRANGLE, SALT LAKE AND DAVIS COUNTIES, UTAH

by Adam P. McKean and Michael D. Hylland

GEOLOGIC MAP OF THE SALTAIR NE QUADRANGLE, SALT LAKE AND DAVIS COUNTIES, UTAH

by Adam P. McKean

INTRODUCTION

This booklet accompanies the geologic maps of the Antelope Island South, Baileys Lake, and Saltair NE 7.5′ quadrangles. The mapped area is located west of downtown Salt Lake City and immediately west of the Salt Lake City International Airport, extending to the southeastern shore of Great Salt Lake. The area also includes the southeastern arm of Great Salt Lake, the southern tip of Antelope Island, and southern Farmington Bay. The area contains the northern part of the Kennecott Utah Copper, LLC tailings impoundments, Interstate 80, agriculture and pasture land, the International Center commercial area, the site of the under-construction Utah State Prison, part of the Farmington Bay Waterfowl Management Area, landfills, migratory bird refuges, and a number of duck hunting club wetlands.

Plate 2 of this report provides supplemental information for all three geologic maps in the map area. Not all map units are present on each quadrangle (see plate 2). Cross sections A-A″ and B-B″ extend across multiple quadrangles (see plate 2).

PREVIOUS WORK

The Baileys Lake and Saltair NE quadrangles, which do not contain bedrock exposed at the surface, have not been mapped at a scale of 1:24,000. Miller's (1980) surficial geologic map at a scale of 1:100,000 includes the area covered by these quadrangles.

The Antelope Island South quadrangle is composed of three parts: southern Antelope Island, Great Salt Lake, and the southeast shore area adjacent to the Baileys Lake quadrangle. The bedrock geology of Antelope Island was first mapped by Larsen (1957) at 1:24,000 scale, then by Graff and others (1980) at 1:48,000 scale. Doelling and others (1990) completed a surficial and bedrock geologic map of Antelope Island at 1:24,000 scale (subsequently published as a geographic information system [GIS] reproduction; see Doelling and others, 2018). The surficial geology of the southeast shore was mapped by Miller (1980) at a scale of 1:100,000. The Doelling and others (1990, 2018) map, with some modifications to the surficial and bedrock geology, was our source for mapping the bedrock of the Antelope Island South quadrangle.

GEOLOGIC SUMMARY

The geology of the Antelope Island South, Baileys Lake, and Saltair NE quadrangles consists primarily of Quaternary surficial lacustrine, deltaic, alluvial, and marsh deposits. Bedrock is only exposed on the south part of Antelope Island (see the northern part of the Antelope Island South quadrangle). Antelope Island bedrock includes truncated Precambrian to Paleozoic and Tertiary sections (Doelling and others, 1990, 2018; Willis and Jensen, 2000; Yonkee and others, 2000a, 2000b; Willis and others, 2010), but the Antelope Island South quadrangle has only Precambrian and Tertiary bedrock.

Bedrock Stratigraphy and Geologic Structure

The oldest rocks in the map area include seven informal units of the Paleoproterozoic Farmington Canyon Complex (Yonkee and others, 2000a): (1) layered gneiss, (2) quartz-rich gneiss, (3) metamorphosed ultramafic rock, (4) banded gneiss, (5) granite and pegmatite, (6) chloritic gneiss, and (7) phyllonite and mylonite. The chloritized and hematitized gneiss, mylonite and phyllonite map units of Doelling and others (1990, 2018) is equivalent to the chloritic gneiss and phyllonite, and mylonite map unit of Yonkee and others (2000a). Yonkee (1990) and Yonkee and others (2000a) reported that these units experienced greenschist retrograde metamorphism and shearing during Mesozoic thrusting and subsequent exhumation. Clark and others (2017) mapped them as Cretaceous-age, retrograde altered and deformed rocks of the Paleoproterozoic Farmington Canyon Complex (KXa). Other Precambrian and Paleozoic rocks found elsewhere on Antelope Island (Doelling and others, 1990, 2018; Yonkee and others, 2000b) are not exposed on the Antelope Island South quadrangle. On the east side of Antelope Island, the Tertiary Salt Lake Formation unconformably overlies the Farmington Canyon Complex (Doelling and others, 1990, 2018; Willis and Jensen, 2000). Away from Antelope Island, several deep drill holes intercept bedrock similar to that exposed on Antelope Island.

The Farmington Canyon Complex rocks record a complex history of igneous intrusion, partial melting, high-grade metamorphism, and deformation (Hedge and others, 1983; Bryant 1988; Yonkee and others, 2000a; Willis and others, 2010). The protolith of the Farmington Canyon Complex is likely an Archean (?) supracrustal sequence of sedimentary strata. These strata experienced Neoarchean (?) metamorphism and deformation prior to main-phase deformation which included the layered gneiss and quartz-rich gneiss. Paleoproterozoic granitic intrusions, main-phase metamorphism of upper amphibolite to granulite facies, and deformation produced the layered gneiss, quartz-rich gneiss, and ultramafic rock. Partial melting during this stage also produced pegmatite dikes and migmatite. Following peak metamorphism and deformation, Proterozoic intrusion of late-stage granite crosscuts main-phase foliation (Yonkee and others, 2000a). Nonconformable Neoproterozoic to Mesozoic deposition of sedimentary rocks followed; these rocks are preserved on the northern part of Antelope Island (Yonkee and others, 2000b), but they are not exposed on the Antelope Island South quadrangle (see Doelling and others, 1990, 2018). The altered and deformed rocks (KXa) of the Farmington Canyon Complex record the deformation and greenschist retrograde metamorphism that occurred during the emplacement of large thrust sheets in the region during the Cretaceous Sevier orogeny (Yonkee, 1990; Yonkee and others, 2000a). Structural analysis and schematic regional cross sections suggest the bedrock of Antelope Island is in the footwall of the Willard thrust and hanging wall of the Ogden thrust (Yonkee, 1992; Willis and Jensen, 2000; Willis and others, 2010; Clark and others, 2017).

The Precambrian bedrock on Antelope Island is separated from Paleozoic bedrock to the south of the study area in the Oquirrh Mountains by an inferred east-west-trending transverse fault zone mapped by Clark and others (in review). The age, configuration, and movement direction on this fault zone is uncertain, but its existence is based on regional changes in stratigraphy and structural fabric in part of the Sevier thrust belt (Clark and others, in review).

Advancing thrust sheets and orogenic highlands shed large amounts of sediment during the Late Cretaceous to middle Eocene. To the south, Eocene to Oligocene magmatism produced volcanic deposits and volcaniclastic sediment (Biek and others, 2005, 2007, 2018; Solomon and others, 2007, 2018; McKean, 2014; Clark and others, 2017). Synorogenic and igneous-related deposits unconformably overlie Precambrian to Mesozoic bedrock in the region. Large-displacement extensional normal faults during the Miocene to Holocene created the current basin and range-type topography. Slip along extensional faults formed the horst block of bedrock that is Antelope Island and Tertiary-Quaternary sediment filled grabens present in all three quadrangles (Bortz and others, 1985; Viveiros, 1986; Wilson and others, 1986; Lambert and West, 1989; McNeil and Smith, 1992; Petropoulos, 1994; Mohapatra, 1996). The Salt Lake Formation on the east side of Antelope Island was deposited in one of these Tertiary basins beginning in the Miocene between 11 and 8 Ma (Willis and Jensen, 2000).

Extension is still occurring on basin and range normal faults of the Intermountain Seismic Belt. The main trace of the Wasatch fault zone is east of the study area (see Personius and Scott, 1992; Nelson and Personius, 1993; and McKean, 2014). Within the study area the Antelope Island segment of the Great Salt Lake fault zone located west of Antelope Island has evidence of Holocene surface faulting (see Colman and others, 2002; Pechmann and Dinter, undated; Dinter and Pechmann, undated; Dinter and Pechmann, 2014; and Clark and others, 2017). Part of the West Valley fault zone, antithetic to the Wasatch fault zone (Keaton and others, 1987; Keaton and Currey, 1989; Hylland and others, 2014), is present in the eastern part of the Baileys Lake quadrangle. These faults are discussed in detail in the "Selected Geologic Hazards" section.

Surficial Geology

Surficial geologic deposits in the map area consist of Quaternary lacustrine, deltaic, alluvial, and marsh deposits. Lacustrine and deltaic sediments were deposited by late Pleistocene Lake Bonneville (30 to 13 ka), the Gilbert-episode lake (~11.5 ka), and Holocene Great Salt Lake (since ~11 ka) (see table 1; unless noted, all ages are in calibrated years). Following Oviatt (2014), the Gilbert-episode lake is regarded as a separate lake rather than a phase of the Bonneville or Great Salt Lake cycles. The Gilbert-episode deposits and shoreline are exposed at elevations below about 4250 feet (~1295 m), with no evidence of Gilbert-episode shorelines above that el-

Table 1. *Ages of major shoreline occupations of Lake Bonneville, Gilbert-episode lake, and Great Salt Lake and shoreline elevations in the Antelope Island South, Baileys Lake, and Saltair NE quadrangles.*

Lake Cycle and Phase	Shoreline (map symbol)	Age		Elevation feet (meters)
		radiocarbon years (^{14}C yr B.P.)	calibrated years (cal yr B.P.)[1]	
Lake Bonneville				
Transgressive phase	Stansbury (S) shorelines	22,000–20,000[2]	26,000–24,000	4440–4490 (1353–1369)
	Bonneville (B) flood	~15,000[3]	~18,000	5220–5250 (1591–1600)
Overflowing phase	Provo (P)	15,000–12,600[4]	18,000–15,000	4860–4880 (1481–1487)
Regressive phase	Regressive shorelines	12,600–11,500[4]	15,000–13,000	not mapped
Gilbert-episode lake	Gilbert (G)	10,000[5]	11,500	4245–4260 (1293–1298)
Great Salt Lake				
	early Holocene highstand	9700–9400[6]	11,000–10,500	4225–4230? (1288–1289)
	late Holocene highstand (H)	4200–2100[7]	5000–2000	4217–4221 (1285–1287)
	historical highstand (h)		late 1860s to early 1870s and 1986–87[8]	4212 (1284)

[1] All calibrations made using OxCal ^{14}C calibration and analysis software (version 4.3.2; Bronk Ramsey, 2009; using the IntCal13 calibration curve of Reimer and others, 2013), rounded to the nearest 500 years. B.P. = before present, meaning the number of years before A.D. 1950

[2] Oviatt and others (1990)

[3] Bonneville shoreline highstand duration may have been shorter than our rounding error of 500 years; age represents lake culmination (Oviatt, 2015; Miller, 2016; and references therein)

[4] See Godsey and others (2005, 2011), Oviatt (2015), and Miller (2016) for the timing of the occupation of the Provo shoreline and subsequent regression of Lake Bonneville to near Great Salt Lake level. Data in Godsey and others (2005) may suggest that regression began earlier, shortly after 16.5 cal ka (see sample Beta-153158, with an age of 13,660 ± 50 ^{14}C yr B.P. [16.5 cal ka] from 1.5 m below the Provo shoreline). Also, lacustrine carbonate deposits in caves reported by McGee and others (2012) seem to support an earlier Lake Bonneville regression beginning around 16.4 cal ka.

[5] Gilbert-episode highstand may have been very short lived; age represents lake culmination (Oviatt and others, 2005; Oviatt, 2014)

[6] Murchison (1989), Currey and James (1982)

[7] Miller and others (2005)

[8] Arnow and Stephens (1990)

evation, which is consistent with Oviatt (2014). The mapped Great Salt Lake historical highstand shoreline "h" is at or below the superelevated shoreline mapped by Atwood (2006) on Antelope Island. Holocene Great Salt Lake ooids are common in and near the lake and are discussed in greater detail in the "Ooids" subsection.

A thin loess conceals many of the deposits in the area. In some exposures a weak buried soil divides the loess into upper and lower parts. Optically stimulated luminescence (OSL) dating of upper and lower loess deposits at the Baileys Lake paleoseismic trench site yielded ages of 3.2 ± 0.5 ka and 12.5 ± 1.4 ka, respectively (Hylland and others, 2012, 2014). The loess in these trenches probably correlates with the loess observed in hand-dug auger holes in the map area. The presence of loess in the auger holes was used to distinguish between older deposits (Pleistocene and Holocene) that predate the loess and younger deposits (Holocene) that postdate the loess (see note in figure 1).

A number of active (Holocene) geologic hazards are mapped in the quadrangles, including landslide deposits (Qms) and surface fault ruptures (scarps). These geologic hazards are described and discussed in more detail in the "Selected Geologic Hazards" section.

Ooids

Ooids are carbonate-coated grains that formed (and continue to form) in the hypersaline, carbonate-saturated Holocene Great Salt Lake and are found in a number of surficial geologic units in the map area (Qlgy, Qlmy, Qlpm, Qlos, and Qly). Wave and wind action transports ooids along the lake shore and periodic flooding of Great Salt Lake has transported ooids inland.

Previous authors have researched many aspects of Great Salt Lake and Lake Bonneville ooids including their origin, formation, and age (for example, Mathew, 1930; Eardley, 1938; Kahle, 1974; Sandberg, 1975; Halley, 1977; Folk, 1993; Folk and Lynch, 2001; Pedone and Norgauer, 2002; Rey, 2012; McGuire, 2014; and Paradis and others, 2017). Traditionally ooids are difficult to date because they form episodically by adding laminae over time and can have long time intervals without carbonate formation. Radiocarbon dating of a single ooid or group of ooids represents the average laminae formation age of a grain or group of grains that may have formed over hundreds to thousands of years. To constrain timing of ooid formation in Great Salt Lake, samples of oolitic sand from unit Qlos (table 2, RC1 on Antelope Island South) were collected and radiocarbon dated (McKean and others, 2016). Ooids were dated using a method described by Duguid and others (2010) and McGuire (2014) that attempts to date the ooid laminations from cortex to core in steps, instead of dating the ooid as a whole. The carbonate outer cortex and inner core group of laminae (not including the core or nuclei material) of our samples were radiocarbon dated to better determine the minimum and maximum formation age of the ooid over time. Samples of ooids (unit Qlos) from the Antelope Island South quadrangle (table 2) formed between 6000 and 7500 cal yr B.P. (McKean and others, 2016). Great Salt Lake ooid ages in McGuire (2014) from Bridger Bay, on the north side of Antelope Island, have a roughly 6000-year (radiocarbon) age span (8144 to 2024 ^{14}C yr B.P.). Ooids from Rozel Point on the north shore of Great Salt Lake had an average age of 500 ^{14}C yr B.P. (McGuire, 2014). The different ages of ooid formation show a time frame that spans the upper and middle Holocene. The large age range is expected since Great Salt Lake water level has oscillated numerous times in the Holocene and the lake has usually been saturated with carbonate, resulting in locations having adequate conditions for ooid formation at different time periods.

Drill Hole Data

Very little bedrock is exposed at the surface within the map area. A combination of exploration drill holes/wells, water wells, gravity data, and seismic data discussed below provide vital data for interpreting the subsurface geology. For a summary and location of the exploration wells and select water wells described below see tables 3 and 4 and plate 1 for each map. Seismic data are discussed in a subsequent section.

In the Antelope Island South and Baileys Lake quadrangles, three drill holes (DH1, DH5, and DH6) penetrated Precambrian bedrock. Pre-Tertiary bedrock was not penetrated by several drill holes in the eastern part of the Baileys Lake quadrangle but Mesozoic and Paleozoic strata may be present under much of the eastern part of the quadrangle based on the geology of exposed bedrock and drill holes outside of the quadrangle (Van Horn, 1981; Bryant, 1988, 1990; Solomon and others, 2007, 2018; McKean, 2014). Exposed geology in adjoining quadrangles implies that several major Sevier-age thrust faults are present in the Precambrian to Mesozoic strata in the subsurface. The location and exact nature of these structures are uncertain (figure 2 in Yonkee, 1992; figure 3 in Willis and Jensen, 2000; figure 2 in Willis and others, 2010; Clark and others, 2017; Clark and others, in review).

Saltair #1 (DH5)

In the Baileys Lake quadrangle, the geophysical log of the Saltair #1 well (table 3) indicates that the Quaternary-Tertiary contact is at a depth of 1288 feet (393 m) and the Tertiary-Precambrian contact is at a depth of 3070 feet (936 m) (Willis and Jensen, 2000).

Saltair #2 (DH6)

In the Baileys Lake quadrangle, geophysical and geologic logs for the Saltair #2 well (table 3) place the top of the Tertiary at a depth of 1086 feet (331 m). Two boxes of core labeled as 1721

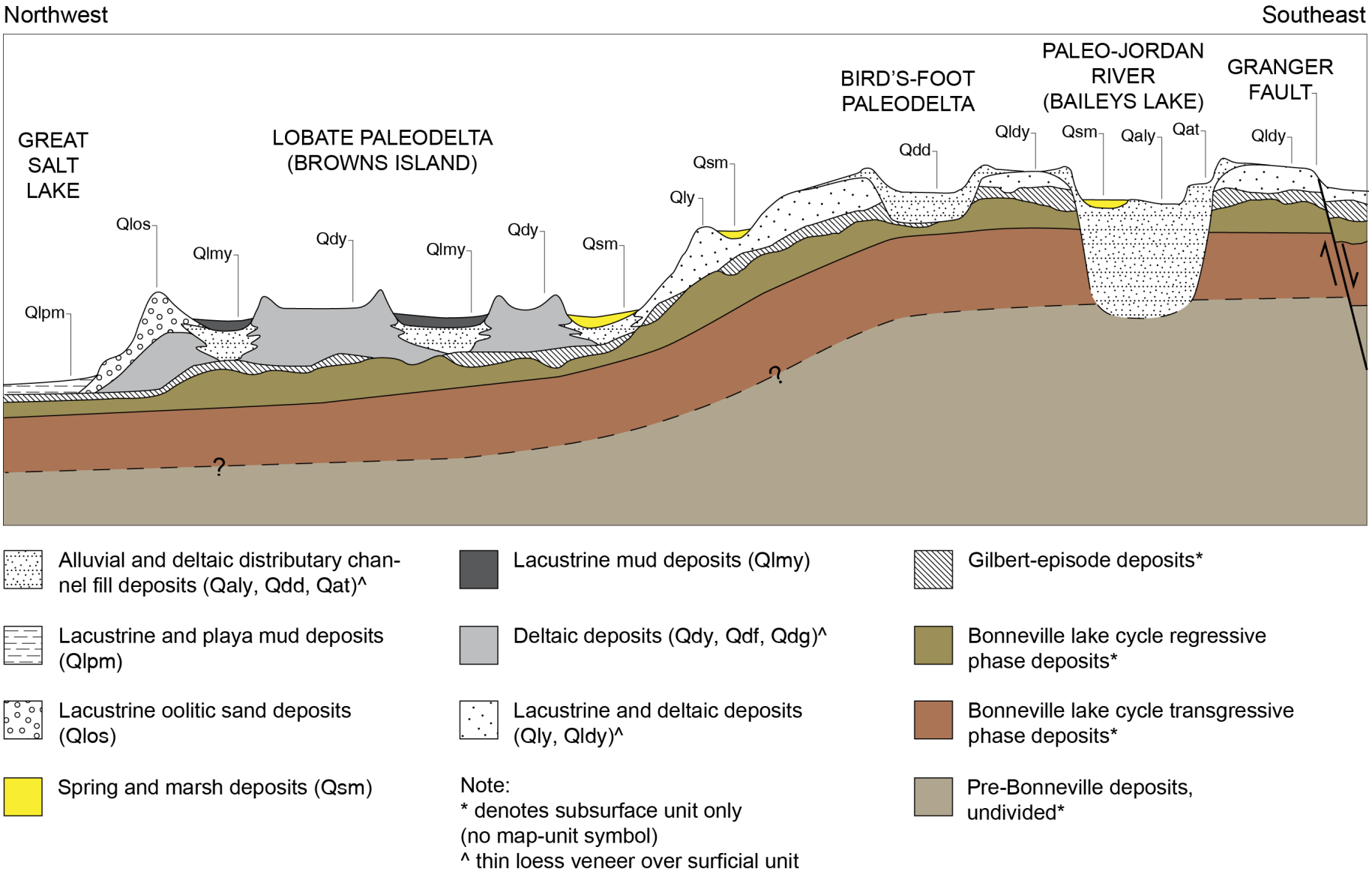


Figure 1. *Schematic northwest-southeast cross section of surficial geology based on auger holes hand-dug to supplement the geologic mapping across the easternmost part of the Antelope Island South quadrangle and the Baileys Lake quadrangle. Cross section shows vertically exaggerated lateral and subsurface relations of geologic units. Not to scale, for reference only.*

Table 2. Summary of radiocarbon age analyses from the Antelope Island South quadrangle.

Map No.	Sample No.	Latitude (°N)	Longitude (°W)	Reference	Notes	Age Data Summary
RC1	SLCN2014–278	40.80787	112.13103	McKean and others, 2016	3 ooid sand samples and 1 bulk soil sample	Averaged calibrated radiocarbon age for ooid formation is between 6000 and 7500 cal yr B.P., calibrated radiocarbon age of organic material in the soil developed on the lower ooid deposit had an average calibrated age of 344 ± 15 cal yr B.P. (see text and figure 3 for discussion)

Notes:
Map number corresponds to sample identification on Antelope Island quadrangle
Location based on NAD83

to 1740-foot (525–530 m) and 3200 to 3207-foot (975–977 m) intervals both contain consolidated rock that appears to be Precambrian high-grade metamorphic bedrock (Willis and Jensen, 2000). Willis and Jensen (2000) suggested the box listing shallower depths is likely mislabeled and estimated the Tertiary-Precambrian contact to be below the 3000-foot interval. The total depth of the well is 3207 feet (977 m). Our review of the basin configuration, geophysical well logs, and the Saltair #1 well confirms their conclusion.

Whitlock-Morton Salt Co. #1 (DH1)

In the Antelope Island South quadrangle, the geophysical log of the Whitlock-Morton Salt Co. #1 well (table 3) indicates the top of the Tertiary is at 1430 feet (426 m), and that the Tertiary section is composed of unconsolidated sediments with approximately 300 feet (~100 m) of interleaved volcanic rock within the 2300 to 2800-foot (700–850 m) depth interval. The volcanic interval is dated at 34 to 37 Ma (late Eocene) (Willis and Jensen, 2000). These strata may include a thin interval of Miocene Salt Lake Formation (Arnow and Mattick, 1968) at the top of the section. Arnow and Mattick (1968) and Willis and Jensen (2000) reported the top of high-grade metamorphic Precambrian rock at 3650 feet (1113 m) and a conglomerate at 4126 feet (1258 m), which could be interpreted as a normal sequence of Precambrian rocks or, alternatively, a younger conglomerate in the footwall of a thrust. The total depth of the well is 4231 feet (1290 m).

Other wells

Two water wells (see table 4) south of the Antelope Island South quadrangle in the Farnsworth Peak quadrangle encountered what are likely Paleozoic units. Water well 427887 (table 4) encountered valley fill to 475 feet (145 m) followed by limestone and quartzite to a drill depth of 485 feet (148 m) (Clark and others, 2017). Water well 12621 (table 4) encountered valley fill to 882 feet (269 m) and limestone to a drill depth of 886 feet (270 m) (Clark and others, 2017). The presence of subsurface Paleozoic rocks south of the Precambrian rocks supports the position of the inferred east-west-trending transverse fault zone between the Precambrian bedrock of Antelope Island and the Paleozoic bedrock of the Oquirrh Mountains (Clark and others, in review).

Two water wells (see table 4) north of our study area on the southeast side of Antelope Island penetrated Quaternary, Tertiary and Precambrian units. The western water well (table 4), and the shallower of the two, encountered Tertiary conglomerate strata at 100 feet (30 m). Precambrian gneiss and granitic bedrock were encountered from 500 feet (152 m) to 600 feet (183 m) (Willis and Jensen, 2000). The eastern water well (table 4) encountered Tertiary Salt Lake Formation at 100 feet (30 m) and Tertiary conglomerate strata from 1200 feet (366 m) to 2082 feet (635 m); the rock type at total depth is inconclusive but the hole may have bottomed in metamorphic rock (Willis and Jensen, 2000). A calculated dip of about 40° E. for the Tertiary units is consistent with the average range of 20° to 45° dips of Tertiary outcrop on the east side of Antelope Island (Doelling and others, 1990, 2018; Willis and Jensen, 2000).

Sediment cores

A number of regionally correlated tephras were previously identified in two sediment cores (SC1, SC2) in the southern half of the Baileys Lake quadrangle. In the Saltair core (SC1, table 5) previous authors identified and correlated the Natural Trap(?), Lava Creek B (0.64 Ma), and Bishop ash (0.759 Ma) beds (Eardley and Gvosdetsky, 1960; Eardley and others, 1973; Williams, 1994). In the S28 core (SC2, table 5) previous authors identified and correlated the Natural Trap(?), Lava Creek B, Ranch Canyon, Rye Patch Dam, and Bishop ash beds (Eardley and others, 1973; Williams, 1994; Lanphere and others, 2002). While not used to create the cross section, these ash beds provide a calibration for depth to these regionally important Quaternary ash bed deposits.

Seismic Data

Baileys Lake

In the Baileys Lake quadrangle, a mostly east-west seismic refraction section collected by the U.S. Geological Survey

Table 3. *Summary of oil and gas exploration drill holes/wells from the Antelope Island South and Baileys Lake quadrangles and other quadrangles near the map area.*

Map Number	API Number	Well Name	Company	Year Completed	7.5' Quadrangle	Latitude (°N)	Longitude (°W)	Total Depth ft (m)	Lithology Notes
DH1	4303511442	Whitlock-Morton Salt Co 1	Whitlock, L E	1956	Antelope Island South	40.80631	112.13131	4231 (1290)	Quaternary 0 ft, Tertiary 1432 ft, Oligocene-Eocene volcanics 2330–2807 ft, Tertiary clastics? 2807–3654 ft, Precambrian metamorphics 3654 ft -TD (Ritzma, unpublished data UGS files, 1975; Willis and Jensen, 2000)
DH2	4303500002	Idras 1	DOSECC Exploration Services, LLC	2016	Baileys Lake	40.81634	112.10092	665 (203)	Test well, Quaternary to TD
DH3	4303516540	Jonnie Fee 1	Geotronic Development Co	1959	Baileys Lake	40.79658	112.00159	565 (172)	Quaternary to TD
DH4	4303516542	Frost 1	Byrd-Frost Inc	1951	Baileys Lake	40.85080	112.05632	1916 (584)	Quaternary? to TD
DH5	4303530002	Saltair 1	Mountain Fuel Supply Co	1975	Baileys Lake	40.78945	112.09911	3265 (995)	Quaternary 0 ft, Tertiary 1228 ft, Precambrian 3070 ft (Willis and Jensen, 2000)
DH6	4303530003	Saltair 2	Mountain Fuel Supply Co	1975	Baileys Lake	40.81804	112.0798	3207 (978)	Quaternary 0 ft, Tertiary 1086 ft, unreliable data for TD (Willis and Jensen, 2000)
DH7	4303530005	Gillmor 3	Pease Oil and Gas Company	1976	Baileys Lake	40.79176	112.05118	2119 (676)	Quaternary 0 ft, Tertiary? 1048 ft
*	4304530010	ST of UT N 1 (Sandbar)	AMOCO Production Company	1980	Plug Peak SE	40.75522	112.30556	7864 (2398)	Paleozoics at ~6600 ft to TD (Bortz and others, 1985)
*	4301130002	ST of UT E 1 (Antelope Island)	AMOCO Production Company	1979	Plug Peak NE	40.97917	112.34907	10,419 (3176)	Pleistocene 0 ft, Pliocene ~3000 ft, Miocene ~4500 ft, Precambrian ? ft - TD (Bortz and others, 1985; Bortz, 2002)

Notes:
Data from Utah Division of Oil, Gas and Mining (UDOGM) database (https://oilgas.ogm.utah.gov/oilgasweb/live-data-search/lds-logs/logs-lu.xhtml, accessed March 10 and 16, 2017)
* indicates location is not in the mapped area
Location data based on NAD83
Lithology notes compiled from UDOGM files and other sources
TD = total depth

Table 4. *Summary of selected water wells from near the mapped area.*

Well ID No.	Water Right	Well Type	Owner	Year Completed	7.5' Quadrangle	Latitude (°N)	Longitude (°W)	Total Depth ft (m)	Lithology Notes
427887	59-1745	water well	SITLA (GSL Marina)	1966	Farnsworth Peak	40.73554	112.21208	485 (148)	Valley fill to 475 ft, limestone and quartzite to TD
12621	59-1196	water well	Kennecott Utah Copper	1964	Farnsworth Peak	40.73567	112.17269	886 (270)	Valley fill to 882 ft, limestone to TD, well abandoned
32548	31-4285	water well	State of Utah Division of Parks & Recreation[1]	1976	Antelope Island	See footnote[2]		2082 (635)	Late Quaternary to 100 ft, Tertiary Salt Lake Fm to 1200 ft, Tertiary conglomerate to TD (Willis and Jensen, 2000)
--	31-4483	water well	State of Utah Division of Parks & Recreation[1]	1977	Antelope Island	See footnote[3]		600 (183)	Late Quaternary to 100 ft, Tertiary conglomerate to 550 ft, Precambrian gneissic and granitic bedrock to TD (Willis and Jensen, 2000)

Notes:
Data from Utah Division of Water Rights database (https://www.waterrights.utah.gov/wellInfo/wellInfo.asp, accessed October 30, 2017)
Water well locations are approximate, location based on NAD83
TD = total depth
[1] Well previously owned by Antelope Island Cattle Company, Inc. (part of the Anchutz Corporation)
[2] Approximate location N. 1650 ft and W. 100 ft from the SE Corner Section 33, T. 3 N., R. 3 W., SLBLM (S.B. Montgomery, Utah Division of Water Resources, written memorandum, 1980, in Willis and Jensen, 2000)
[3] Approximate location N. 1600 ft and W. 2300 ft from the SE Corner Section 33, T. 3 N., R. 3 W., SLBLM (S.B. Montgomery, Utah Division of Water Resources, written memorandum, 1980, in Willis and Jensen, 2000)

Table 5. *Summary of sediment cores and tephrochronology data from the Baileys Lake quadrangle.*

Map No.	Core Name	Date Cored	7.5' Quadrangle	Latitude (°N)	Longitude (°W)	Total Depth ft (m)	Tephra Name	Depth[1] (ft.in)	Depth (m)	Correlation Age (Ma)	Reference
SC1	Univ. of Utah Saltair	prior to 1960	Baileys Lake	40.7879	112.1247	650 (198)					Eardley and Gvosdetsky, 1960; Eardley and others, 1973; Williams, 1994
							Lava Creek B	547.6	166.9	0.64	
							Bishop	646.0	196.9	0.759	
SC2	Univ. of Utah S28	1960s	Baileys Lake	40.7869	112.0687	765 (233)					Eardley and others, 1973; Williams, 1994
							Natural Trap?	112.9	34.4	0.11*	
							Lava Creek B	467.9	142.6	0.64	
							Ranch Canyon	505.4	154.0		
							Rye Patch Dam	505.8	154.1		
							Bishop	574.6	175.1	0.759	

Notes:

Map number corresponds to sample identification on Baileys Lake quadrangle

Core locations are approximate, location data based on NAD83

Age type (correlation age) is based on geochemical correlation to the database of analyses/stratigraphic data/age dates for late Cenozoic vitric tephra layers in the Western U.S. assembled by M.E. Perkins and several colleagues at the University of Utah, Dept. of Geology and Geophysics. Refer to Williams (1994) for procedures on sample preparation and analyses. For correlation ages see Williams (1994) and Lanphere and others (2002)

[1] Depth is in feet plus inches (ft.in), for example a depth of 547 feet and 6 inches is shown as 547.6 using the abbreviation of Williams (1994)

* indicates an estimated age in Burmester core (Williams, 1994)

shows thicknesses and depths of Quaternary deposits, Tertiary deposits, and consolidated rocks (Arnow and Mattick, 1968). Well logs (lithologic and electrical) from exploration oil and gas wells were used in combination with an east-west seismic reflection line (R–11) across the Antelope Island South, Baileys Lake, and Salt Lake City North quadrangles (Radkins and others, 1989; Hill and others, 1990) to help determine the subsurface contacts between Quaternary deposits (unconsolidated sediments), Tertiary strata (semiconsolidated to consolidated strata), Mesozoic to Paleozoic strata (consolidated strata), and basement bedrock (possibly Farmington Canyon Complex).

Farmington Bay of Great Salt Lake

The Precambrian rock and Tertiary deposits identified by bedrock outcrops and the two water wells on southeastern Antelope Island can also be identified on seismic reflection profiles from Elf Aquitaine Petroleum and interpretations were made by Wilson and others (1986) and McNeil and Smith (1992). These authors interpret a bedrock high (or buried horst) beneath southern Farmington Bay, east of southern Antelope Island. The subsurface horst is bounded on the east and west by normal faults. The western fault shows down-to-the-west movement and is interpreted to offset Quaternary and Tertiary sediments to a depth of 7000 feet (2100 m). The eastern faults show down-to-the-east movement with a deeper basin (14,000 feet [4200 m]) lying east of the seismic line nearer the Wasatch fault zone. In seismic reflection data collected by the U.S. Geological Survey, Lambert and West (1989) identified on their profile G-G′ a consolidated high east of southern Antelope Island with inferred down-to-the-west faulting, likely the same down-to-the-west normal fault interpreted by Wilson and others (1986) and McNeil and Smith (1992).

South arm of Great Salt Lake

North of the Antelope Island South quadrangle, an Amoco drill hole and seismic section (line 39) west of Antelope Island and west of the Great Salt Lake fault zone is interpreted to show an approximately 10,000-foot-deep (3000 m) Quaternary to Miocene basin (Bortz and others, 1985; Viveiros, 1986; Petropoulos, 1994; Mohapatra, 1996; Bortz, 2002). Based on the geologic and geophysical log of the Antelope Island well (State of Utah E–1, table 3) located just north of this seismic section, Precambrian metamorphic rocks were encountered at 9250 feet (2819 m) to 10,419 feet (3176 m). The geologic and geophysical log available for an Amoco drill hole called Sandbar (State of Utah N–1, table 3), to the south of the seismic section, encountered Quaternary to Miocene units having a thickness of approximately 6600 feet (2012 m). Beneath this is a series of fractured Paleozoic limestones at 7600 feet (2316 m) and 7643 (2329 m) to the total depth of 7864 feet (2397 m). This well supports the location of the inferred east-west-trending transverse fault zone between the Precambrian bedrock of Antelope Island and the Paleozoic bedrock of the Oquirrh Mountains (Clark and others, in review).

Shallow seismic reflection profiles have also been collected in the north and south arms of Great Salt Lake to map the extent and length of the main and auxiliary faults of the Great Salt Lake fault zone and the Carrington fault. In 1997 Colman and others (2002) collected seismic reflection data of the faults beneath Great Salt Lake. Additional data were collected by Dinter and Pechman in 1998, 2003, 2006, 2009, and 2010 (see Pechmann and Dinter, undated; Dinter and Pechmann, undated; Dinter and Pechmann, 2014). Along with the seismic reflection profiles, sediment cores were collected adjacent to the fault zones in the hanging-wall deposits (Colman and others, 2002; Dinter and Pechmann, 2005). The faults are described and discussed in more detail in the "Surface Fault Rupture" subsection of the "Selected Geologic Hazards" section.

METHODS

Mapping of surficial deposits by the UGS is based on age and depositional environment or origin. The letters of the map units in order indicate (1) age (geologic period, e.g., Q for Quaternary); (2) primary depositional environment or origin, usually determined from geologic setting, landform or morphology; (3) grain size(s), bedding, or other distinctive characteristics of the deposits; and (4) additional significant information, such as tighter age constraints (Doelling and Willis, 1995). In the Bonneville basin ages are related to the phases of Lake Bonneville or numbered with 1 being the youngest (active) deposit. For example, unit Qal_1 is a Quaternary surficial deposit of alluvial stream origin (al), and the number one indicates it is young and potentially historically active.

Mapping for the project was done on stereographic pairs of aerial photographs from the following sources: black-and-white aerial photographs at approximately 1:20,000 scale from the U.S. Department of Agriculture (USDA) Agricultural Stabilization and Conservation Service (1937, 1971), and natural color aerial photographs at approximately 1:40,000 scale from the USDA National Agriculture Imagery Program (2009). Some contacts were mapped from U.S. Natural Resources Conservation Service (NRCS) (2010) soil maps. The geologic map was made by transferring the geology from the aerial photographs to a GIS database using the programs ArcGIS, VROne, and VRTwo for a target scale of 1:24,000. We mapped some contacts and faults using 1-meter lidar data acquired by the UGS (available from Utah Automated Geographic Reference Center [AGRC], 2011, and OpenTopography, 2011). Aerial-photographic and field mapping of the surficial geologic deposits in the Antelope Island South, Baileys Lake, and Saltair NE quadrangles were completed in 2013. The bedrock geology of Antelope Island South was digitized and modified by Clark and others (2017) from Doelling and others (1990, 2018) and Yonkee and others (2004a). On the Antelope Island South quadrangle, Clark and others (2017) is the source for the mapped location of the Great Salt Lake fault zone. We completed approximately 50 hand-auger boreholes to depths of <1 to 9 feet (<30 cm to 3 m) in the surficial deposits, which helped reveal Holocene and

Pleistocene strata (figure 1) and make correlations with strata exposed and dated in the Baileys Lake paleoseismic trenches on the Granger fault (Hylland and others, 2012, 2014). Table 1 provides time constraints and elevations for many geologic units and is based on features produced by Lake Bonneville, the Gilbert-episode lake, and Great Salt Lake.

The 2017 U.S. Geological Survey topographic map for the Antelope Island South quadrangle lacks bathymetric contours; we digitally added contours from Baskin and Allen (2005) to supplement the topographic map.

We created cross sections A-A″ and B-B″ by combining available subsurface seismic and gravity data from a number of sources (Cook and Berg, 1961; Arnow and Mattick, 1968; Zoback, 1983; Bortz and others, 1985; Viveiros, 1986; Wilson and others, 1986; Lambert and West, 1989; Radkins and others, 1989; Hill and others, 1990; McNeil and Smith, 1992; Yonkee, 1992; Petropoulos, 1994; Mohapatra, 1996; Willis and Jensen, 2000; Bortz, 2002; Willis and others, 2010). We also used well logs (lithologic and electrical) from exploration oil and gas wells (see table 3) and well logs from selected water wells (table 4) to help determine the subsurface contacts between the Quaternary, Tertiary, and pre-Cenozoic bedrock.

SELECTED GEOLOGIC HAZARDS

The Antelope Island South, Baileys Lake, and Saltair NE quadrangles were mapped to provide the basis for identifying and delimiting potential geologic hazards in future derivative UGS geologic hazard mapping. Geologic hazards in the map area include surface fault rupture, flooding associated with lake level rise, earthquake ground shaking, liquefaction, tectonic subsidence/tilting, debris flow (Qafy), stream flooding (Qal_1, Qaly), waves and flooding associated with earthquakes, shallow groundwater, corrosive soils, and other problem soils. Problem soil units include spring and marsh deposits (Qsm, and Qlam) which also correspond to areas of shallow groundwater, while clay-rich lacustrine and deltaic deposits (Qdy, Qlmy, Qlpm, Qly, and Qldy) may yield soil collapse or expansion problems. Two hazards are briefly discussed below. Additional geologic hazards may exist but are not addressed in this report. We recommend comprehensive site-specific geotechnical and geologic hazard investigations per the guidelines in UGS Circular 122 (Bowman and Lund, 2016). See the UGS website (geology.utah.gov) for additional information on these and other geologic hazards.

Surface-Fault Rupture

Two Holocene-active fault zones are recognized in the study area: the Granger fault of the West Valley fault zone in the Baileys Lake quadrangle, and the Antelope Island segment of the Great Salt Lake fault zone in the Antelope Island South quadrangle.

West Valley fault zone, Granger fault

The north-south-trending West Valley fault zone is partially antithetic to the Salt Lake City segment of the Wasatch fault zone. These two fault zones bound an intrabasin graben in northern Salt Lake Valley. The West Valley fault zone includes the Granger (western) and Taylorsville (eastern) faults. The northern part of the Granger fault is in the Baileys Lake quadrangle.

The Granger fault is a down-to-the-east normal fault approximately 11.5 miles (18.5 km) long end-to-end and is discontinuously exposed in this quadrangle and the adjoining Salt Lake City North and Salt Lake City South quadrangles (McKean, 2014, 2017). The fault scarps are typically 2 to 5 feet (0.5–1.5 m) high with a maximum height of 20 feet (6 m) near the southern end of the Granger fault (Keaton and others, 1987; Keaton and Currey, 1989; Hylland and others, 2014).

Surface traces of the West Valley fault zone (including the Granger fault) were first shown as faults by Marsell and Threet (1960) on their Salt Lake County geologic map. Cook and Berg (1961) correlated the Granger-area faults to a steep gravity gradient in what they called the Jordan Valley graben. Marine and Price (1964) named the faults the Granger and Taylorsville faults of the Jordan Valley fault zone, and provided drill hole data for displacement minimums across the faults. Van Horn's (1979, 1982) 1:24,000-scale surficial geologic maps of the area did not show the fault zone; instead he attributed the scarps to differential erosion of distinct stratigraphic units (Van Horn, 1986, personal communication in Keaton and others, 1987). Miller's (1980) 1:100,000-scale surficial geologic map included the northern part of the Granger fault in the Baileys Lake and Salt Lake City North quadrangles as scarps with uncertain origin. Keaton and others (1987) and Keaton and Currey (1989) conducted the first detailed investigations of the fault zone and confirmed, through geomorphic mapping, trenches, and boreholes, the existence of the Granger and Taylorsville faults. They proposed the West Valley fault zone name for the structure and retained the existing Granger and Taylorsville fault names. Only a few paleoseismic investigations (Keaton and others, 1987; Keaton and Currey, 1989; Hylland and others, 2014, 2017; see plate 2) have been conducted on the fault zone. These studies are discussed below.

Keaton and others (1987) and Keaton and Currey (1989) studied the Granger fault at two localities in the Salt Lake City North quadrangle and three localities in the Salt Lake City South quadrangle. In the Salt Lake City North quadrangle they used boreholes at two localities to determine offset in the subsurface across the Granger fault. One set of boreholes was at the Three Flags locality and the other set was at the Goggin Drain locality (both localities are in section 6, T. 1 S., R. 1 W., Salt Lake Base Line and Meridian [SLBLM]) (Keaton and Currey, 1989). These shallow boreholes identified offset in the near-surface sediment. In the Salt Lake City South quadran-

gle, they used boreholes at two localities to determine offset in the subsurface across the Granger fault. One set of boreholes was at 1300 South near about 4800 West (Keaton and Currey, 1989) and the other set was in a lot at 3166 South 3200 West (Keaton and others, 1987). Keaton and others (1987) excavated two trenches and six boreholes at the Utah Department of Transportation facility near 4501 Constitution Blvd. and identified faulting in the trenches and boreholes (see plate 1 in McKean, 2017). They also conducted geomorphic mapping of cross-cutting relationships between the Granger fault and several post-Bonneville alluvial channels (see figure 6a in Keaton and others, 1987; unit Qaf_{2a} in McKean, 2017; units Qdg and Qafg this report). They characterized deformation along the Granger fault as shear on a typically discrete normal fault plane, as opposed to more monoclinal warping of beds commonly found on the Taylorsville fault (Keaton and others, 1987; Keaton and Currey, 1989). These studies provided definitive evidence for surface-fault ruptures on the Granger fault and long-term (140 kyr) cumulative displacements and slip rates for the West Valley fault zone. However, they were unable to provide individual earthquake timing and displacement data.

In September 2010, the Utah Geological Survey (UGS) excavated trenches to depths of 5 to 10 feet (1.5–3.3 m) across two strands of the Granger fault within the Baileys Lake quadrangle as part of a paleoseismic investigation of the West Valley fault zone (Hylland and others, 2014). The trenches revealed that prehistoric earthquakes on the Granger fault have created 1- to 3-foot-high (0.4–1 m) fault scarps at the Baileys Lake site. The investigation documented four large (surface-faulting) earthquakes since the highstand of Lake Bonneville (~18 ka), the most recent having occurred about 5.5 ka. Although the earthquake timing does not provide an unequivocal coseismic link between the Granger fault and Salt Lake City segment of the Wasatch fault zone, it does suggest that large earthquakes on the West Valley fault zone are likely synchronous with, or triggered by faulting on the Salt Lake City segment (Hylland and others, 2014; DuRoss and Hylland, 2015).

Great Salt Lake fault zone, Antelope Island segment

The Great Salt Lake fault zone, formerly known as the East Great Salt Lake fault, is a west-dipping normal fault zone and set of auxiliary faults submerged beneath Great Salt Lake (Dinter and Pechmann, 2014). The fault zone consists of four segments from north to south: Rozelle, Promontory, Fremont, and Antelope Island. Seismic reflection profiling has been used to map individual fault strands (see Colman and others, 2002; Pechmann and Dinter, undated; Dinter and Pechmann, undated; Dinter and Pechmann, 2014; and Clark and others, 2017). Along with the seismic reflection profiles, sediment cores were collected adjacent to the faults in the hanging-wall and footwall deposits to determine the depositional and displacement history along the fault zone (Colman and others, 2002; Dinter and Pechmann, 2005). The average single-segment earthquake recurrence interval for the Antelope Island and Fremont Island segments was calculated to be 4200 ± 1400 years, based on radiocarbon-dated seismic event horizons (Dinter and Pechmann, 2005). In conjunction with the seismic profiles mentioned above, high-resolution bathymetry (Baskin and Allen, 2005; Baskin and Turner, 2006) was used to define segment boundaries, and to determine the segment fault rupture lengths and scarp heights for the Great Salt Lake fault zone (Dinter and Pechmann, 2014). The fault traces are published on the geologic map of the Tooele 30′ x 60′ quadrangle for the southern part of Great Salt Lake (Clark and others, 2017), which is the source of our data. We modified some traces of the main fault from Clark and others (2017) between seismic lines (see Dinter and Pechmann, 2014) to better match the bathymetry of the lake bed geometry near the north boundary of the Antelope Island quadrangle.

Janecke and Evans (2017) proposed revising the Great Salt Lake fault zone by reinterpreting existing fault segments and adding new fault mapping to create the Oquirrh-Great Salt Lake fault zone (similar to Youngs and others, 1987), with nine segments from north to south: North Promontory, Tarpey, Promontory, Fremont Island, Antelope Island, North Oquirrh, South Oquirrh Mountain, Topliff, and East Tintic Mountain segments. Their interpretation removes the Rozelle segment from the Great Salt Lake fault zone and considers it to be a separate structure called the Rozelle fault zone. In the Antelope Island South quadrangle, the fault traces of Janecke and Evans (2017) coincide with those shown by Clark and others (2017) where the two are crossed by seismic profiles (see Dinter and Pechmann, 2014). Between seismic lines they commonly diverge. Mapping fault scarp locations in a lacustrine setting is problematic even with imagery and bathymetry, as a break in slope (scarp, if fault origin) cannot be directly observed to confirm its tectonic or lacustrine origin. Seismic data are needed to confirm the tectonic origin of a break in slope in a lacustrine setting. On the Antelope Island South geologic map we show seismically confirmed fault traces modified from Clark and others (2017). Just west of the southern tip of Antelope Island, we have also included a modified trace from Janecke and Evans (2017) as an unconfirmed fault trace. The feature (tectonic or lacustrine in origin) was not crossed by previous seismic profiles (see Dinter and Pechmann, 2014) and has a break in slope, according to current bathymetry (Baskin and Allen, 2005), of about 10 feet (3 m). The other mapped faults of Janecke and Evans (2017) were not included on this map because they (1) coincided with those published in Clark and others (2017) at the location where seismic profiles crossed them but diverge from each other away from the seismic lines, (2) did not show a scarp height greater than one foot (0.3 m) in the bathymetry, and/or (3) were crossed by seismic profiles and faulting was not identified (Dinter and Pechmann, 2014). For example, the eastern fault splay of Janecke and Evans (2017) south of Antelope Island is not included because it is crossed by seismic profiles in three separate locations that do not show fault displacement (see Dinter and Pechmann, 2014). Many of Janecke and Evans' (2017) scarps that are not included on this map as faults could represent traces of the

Antelope Island segment, but more seismic work is needed to confirm their fault origin. Bathymetric lidar, if collected in the future, could be used to supplement the seismic data to more accurately delineate, measure, and study this and other potential faults beneath Great Salt Lake.

Lake Flooding

The historical highstand of Great Salt Lake occurred in the late 1860s to early 1870s and again in 1986–87 at an elevation of about 4212 feet (1284 m) (figure 2) (Arnow and Stephens, 1990). As mapped on plate 1, a lake-level rise to the historical highstand shoreline could potentially flood much of the low-elevation valley floor in the quadrangles and elevate shallow groundwater in adjacent areas. For planning and building purposes, land at and below this elevation should not be developed without significant mitigation for a reoccupation of the shoreline by Great Salt Lake. Land above this elevation could still be affected by elevated shallow groundwater level in the event of a lake-level rise and potential storm wave runup along the shoreline during high water years (Atwood and Mabey, 1995; Atwood, 2006).

SUMMARY OF HYDROGEOLOGY

The Baileys Lake, Antelope Island South, and Saltair NE quadrangles are strongly influenced by Great Salt Lake, other surface water, and shallow groundwater. Great Salt Lake occupies a closed basin and has fluctuated tens of feet throughout the Holocene (Murchison, 1989; see table 1). The average elevation of Great Salt Lake is 4200 feet (1280 m), but historical elevations of the lake have been highly variable, ranging from about 4191 to 4212 feet (1277-1284 m). Other water bodies in the map area have higher and varying elevations related to water-control structures used for wetlands mitigation, migratory bird refuges, and duck club ponds. Most groundwater in the map area has high total dissolved solids concentrations (1000 to >10,000 ppm); saline conditions are especially prevalent along the margins of Great Salt Lake (Wallace and Lowe, 2009).

Perched and shallow groundwater conditions exist across much of the map area. In the vicinity of the Baileys Lake fault trenches (Hylland and others, 2014) groundwater monitoring in piezometers documented groundwater to within about 5 feet (1.5 m) of the ground surface during the 2009–10 water year (data available at https://apps.geology.utah.gov/gwdp/; see wells BL-P1 and BL-P2 at the Baileys Lake site). A deep confined aquifer and shallower unconfined aquifer form the principal aquifers for Salt Lake Valley. Many of the water wells in the confined aquifer in the area flow to the surface under artesian pressure. Groundwater flows toward or along the Jordan River, or toward Great Salt Lake (Wallace and Lowe, 2009).

MAP UNIT DESCRIPTIONS

QUATERNARY

Alluvial Deposits

Qal_1 **Modern stream deposits** (upper Holocene) – Moderately sorted, medium- to light-brown sand, silt, and minor clay; very fine to medium-grained sand; contains thin discontinuous sand lenses; subangular to angular sand grains; thin to medium bedded; sand grains include quartz, lithic fragments, and mica flakes; mapped along Lee Creek and downstream of canals along shore of Great Salt Lake; mapped in active channels, floodplains, and on minor terraces less than 5 feet (1.5 m) above active channels; locally includes minor colluvium along steep stream embankments; includes channelized stream deposits and channel embankments; exposed thickness less than 10 feet (3 m).

Qaly **Young stream deposits, undivided** (upper to middle? Holocene) – Moderately sorted, light olive-gray sand, silt, and minor clay; very fine to medium-grained sand; contains thin discontinuous sand lenses; subangular to angular sand grains; thin to medium bedded; sand grains include quartz, lithic fragments, and mica flakes; mapped along the paleo-Jordan River where the river incised down through the young lacustrine and deltaic deposits (Qldy) and formed the depression that hosts Baileys Lake and its associated wetlands (see plate 2); mapped in abandoned meander channels, floodplains, and on minor terraces less than 5 feet (1.5 m) above active channels; locally includes a loess veneer, and minor colluvium along steep stream embankments; includes some channelized stream deposits and channel embankments; includes young lacustrine and alluvial deposits mapped as Qlay by Solomon and others (2007, 2018) in the Magna quadrangle, but not mapped separately in these quadrangles; correlative with younger stream deposits mapped as unit fay by Van Horn (1982) in the Salt Lake City North quadrangle; exposed thickness less than 15 feet (5 m).

Qalg **Stream deposits related to Gilbert-episode lake and/or Great Salt Lake** (middle Holocene? to upper Pleistocene?) – Moderately sorted, light olive-gray sand, silt, and minor clay; very fine to medium-grained sand; contains thin discontinuous sand lenses; subangular to angular sand grains; thin to medium bedded; sand grains include quartz, lithic fragments, and mica flakes; mapped along Interstate 80 near 5600 West; mapped in abandoned channels and floodplains of a stream that once flowed into and through a regressive Gilbert-episode delta (Qdg; plate 2) (Murchison, 1989); could also be related to

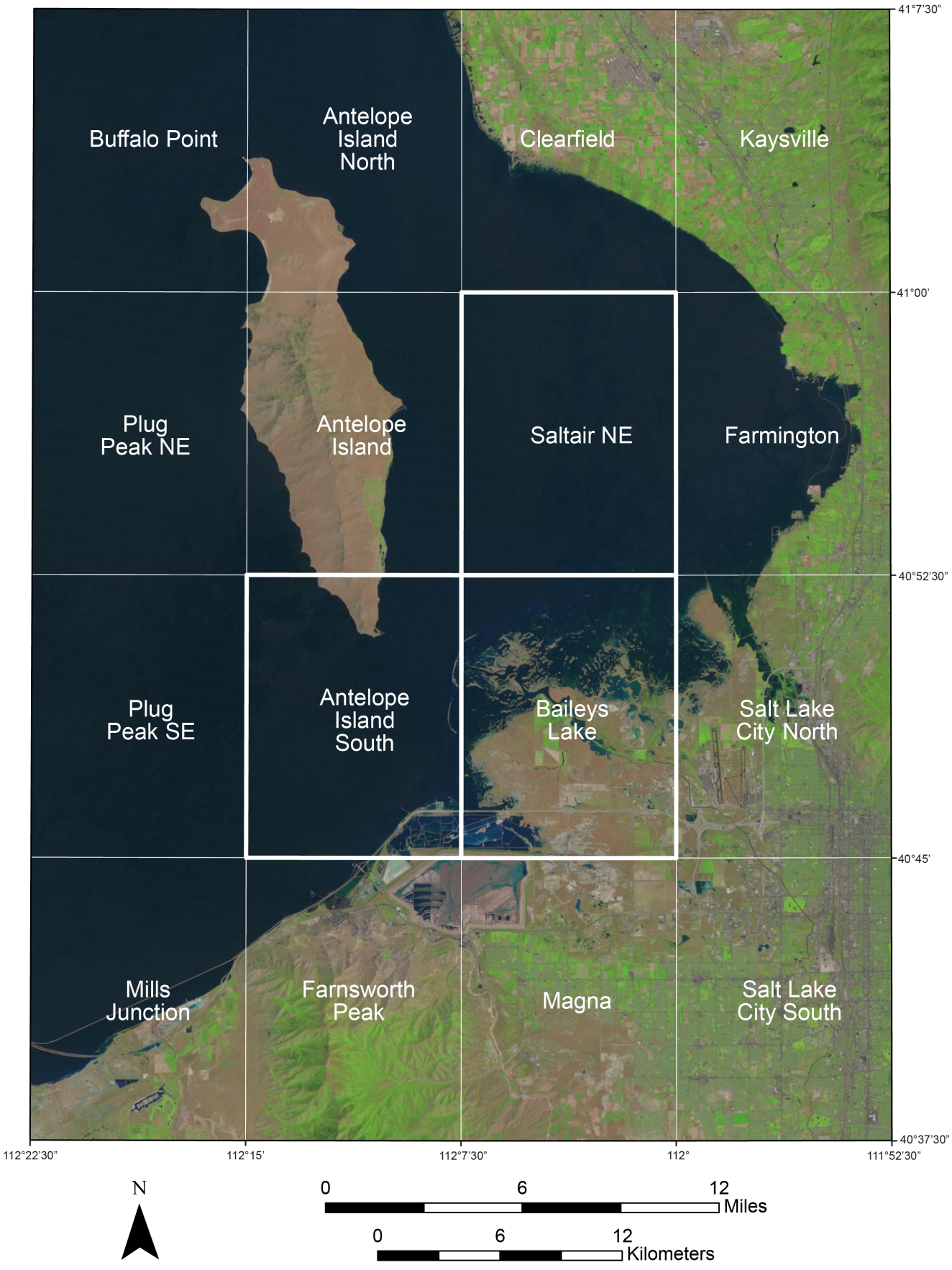


Figure 2. *Cropped Landsat 5 "natural color" image of the flooding that occurred during the 1987 highstand (4212 feet [1284 m]) of Great Salt Lake, showing 7.5' quadrangle boundaries and labels. Image date June 2, 1987. Landsat 5 image courtesy of the U.S. Geological Survey.*

early Holocene highstand of Great Salt Lake based on elevation (see table 1); distinguished from Qdg by the lack of deltaic fans in aerial imagery; unit correlative with Gilbert-episode deltaic deposits in the undivided young deltaic deposits in the Magna quadrangle mapped as Qldy by Solomon and others (2007, 2018), and deltaic deposits mapped as units fdc, fdco, and fdcy by Van Horn (1979, 1982) in the Salt Lake City South and North quadrangles; exposed thickness less than 15 feet (5 m).

Qat **Stream terrace deposits** (upper to middle? Holocene) – Moderately sorted, light olive-gray sand, silt, and minor clay; contains thin discontinuous sand lenses; very fine to medium-grained sand; subangular to angular sand grains; thin to medium bedded; sand grains include quartz, lithic fragments, and mica flakes; mapped on terraces 5 to 15 feet (1.5–5 m) above the paleo-Jordan River channel (Baileys Lake-Goggin Drain area); may include minor alluvial and colluvial deposits from nearby slopes; exposed thickness 15 feet (5 m).

Qafy **Younger alluvial-fan deposits** (Holocene to upper Pleistocene?) – Poorly to moderately sorted pebble to cobble gravel in a matrix of sand, silt, and clay, with boulders, on gentle slopes of Antelope Island; displays thin to thick planar bedding and low-angle cross-bedding; deposited by slope wash, debris flows, debris floods, and streams; mapped on the southwest part of Antelope Island in the Antelope Island South quadrangle; includes alluvial-fan deposits that either have not been differentiated because they are too small to show at map scale or are in areas where the specific age of Holocene deposits has not been determined; postdates regression of Lake Bonneville from the Provo shoreline; estimated thickness less than 30 feet (10 m).

Deltaic Deposits

Qdy **Younger deltaic deposits** (upper to middle? Holocene) – Poorly to moderately sorted, yellowish-brown silt, fine sand, and clay; includes natural levee deposits; sand grains are very fine to medium-grained; subangular to angular sand grains; mapped on the lobate paleodelta that formed at the mouth of the paleo-Jordan River channel near and including Browns Island and a likely younger abandoned Jordan River delta deposit in the northeast corner of the Baileys Lake quadrangle that is mostly contained in the Salt Lake City North quadrangle (McKean, 2014) (plate 2); mapped on an elevated floodplain surface above young lacustrine mud deposits (Qlmy) where natural levee deposits form ridges and run parallel to abandoned river channels and distributary channels; natural levee deposit elevations may coincide with Great Salt Lake intermediate and highstand shorelines; distinguished from young lacustrine and deltaic deposits (Qly and Qldy) by numerous natural levee deposits; locally includes a loess veneer and buried soil; exposed thickness less than 10 feet (3 m).

Qdd **Deltaic distributary channel-fill deposits** (middle to lower Holocene) – Moderately sorted, yellowish-gray to light olive-gray silt with sand and clay; includes natural levee deposits; sand is very fine to fine grained; contains thin discontinuous sand lenses; subangular to angular sand grains; thin to medium bedded; sand grains include quartz, lithic fragments, and mica flakes; located where distributary channels of a bird's-foot-style delta spilled out of the paleo-Jordan River channel southwest of Baileys Lake (plate 2); associated with the late Holocene highstand of Great Salt Lake based on elevation (Murchison, 1989); mapped where delta distributary channels incised down through the young lacustrine and deltaic deposits (Qldy) and deposited channel sediments and their associated natural levee deposits over Qldy; locally includes a loess veneer and buried soil; exposed thickness less than 10 feet (3 m).

Qdf **Deltaic-fan deposits** (middle to lower Holocene) – Moderately sorted, yellowish-gray to light olive-gray silt with interbedded sand and clay; sand is very fine to fine grained; contains thin discontinuous sand lenses; subangular to angular sand grains; thin to medium bedded; sand grains include quartz, lithic fragments, and mica flakes; mapped along the margins of the paleo-Jordan River channel near the Baileys Lake area and between the bird's-foot-style delta distributary channels (plate 2); mapped where bar deposits fill the area between channels and conceal the young lacustrine and deltaic deposits (Qldy), and where crevasse splays breached the meander channel and deposited sediment; locally includes a surficial loess veneer; unit correlates with distributary-channel-fan deltaic deposit mapped as unit fm by Van Horn (1982) in the Salt Lake City North quadrangle; exposed thickness less than 6 feet (2 m).

Qdg **Deltaic deposits related to Gilbert-episode lake and/or Great Salt Lake** (middle Holocene? to upper Pleistocene?) – Moderately to well-sorted, moderate to dark yellowish-brown sand, silt, and minor clay; sand is fine to medium grained; contains thin discontinuous sand lenses; subangular to angular sand grains; thin to medium bedded; sand grains include quartz, lithic fragments, and mica flakes; mapped south of Interstate 80 near 5600 West where older (Gilbert episode and/or early Great Salt Lake) stream deposits (Qalg) fed and eventually flowed through the delta as lake levels fluctuated; mapped where a meander channel (Gilbert-episode paleo-Jordan Riv-

er?) spread out into distributary channels and formed a delta deposit; distinguished from young lacustrine and deltaic deposits (Qldy) by the deltaic fans and channels visible on aerial photography (plate 2); locally includes a surficial loess veneer; unit may be correlative with Gilbert-episode deltaic deposits in the undivided young deltaic deposits (Qldy) in the Magna quadrangle (Solomon and others, 2007, 2018), and distributary-channel-fill deltaic deposits mapped as units fdc, fdco, and fdcy by Van Horn (1979) and Qal_{2a} by McKean (2017) in the Salt Lake City South quadrangle; Gilbert-episode age from Murchison (1989) based on elevation and location but could also be related to Great Salt Lake; exposed thickness less than 6 feet (2 m).

Human-Derived

Qh **Fill and disturbed land** (historical) – Undifferentiated earthen fill and/or disturbed land related to the construction of canals, landfills, tailings impoundment embankments, water control structures used for wetlands mitigation, migratory bird refuges, and duck club ponds, and fill used for construction of Interstate Highway 80 and 215 and railroad lines; includes construction debris in landfills near 7200 West; only the larger areas of disturbed land are mapped, and many areas in these maps have been regraded and developed and may contain unmapped deposits of fill; the tailings embankment in the southwest corner of the Baileys Lake quadrangle and southeast corner of the Antelope Island South quadrangle is composed of coarse-grained tailings (Rio Tinto, undated); the tailings embankment is 125 to 250 feet thick (40–75 m), but other fill thickness is probably less than 50 feet (15 m).

Qht **Tailings** (historical) – Tailings from the active and historical mining operations associated with Kennecott/Rio Tinto operations; mapped in large impoundments in the southwest corner of the Baileys Lake quadrangle and southeast corner of the Antelope Island South quadrangle and are composed of finer grained tailings (Rio Tinto, undated); a smaller disposal site is mapped northeast of the large active impoundment.

Lacustrine Deposits

Qlb **Lacustrine boulders** (Holocene? to upper Pleistocene) – Boulders deposited along beach and shoreface of Lake Bonneville, Gilbert-episode lake, and Great Salt Lake, where fines have been removed by erosion; boulder fields are only mapped on bedrock knobs and strandlines of Antelope Island (after Doelling and others, 1990, 2018); not differentiated by age; thickness as much as 10 feet (3 m).

Qlg **Lacustrine gravel and sand** (Holocene to upper Pleistocene) – Moderately to well-sorted gravel and sand with minor silt, oolitic sand, and boulders; clasts are typically well rounded and sorted (Clark and others, 2017); thin to thick bedded; mapped as veneers over bedrock; ooids are located in the lower elevation deposits that are below the Great Salt Lake Holocene highstands (see table 1); only mapped on Antelope Island at and below the Provo shoreline, includes both transgressive and regressive Lake Bonneville, Gilbert-episode lake, and Great Salt Lake deposits; not differentiated by age; thickness variable, 0 to 100 feet (0–30 m).

Qlgy **Young lacustrine gravel and sand** (Holocene) – Moderately to well-sorted gravel and sand, includes oolitic sand, carbonate chips and clasts, and minor silt; quartz and lithic sand grains are angular to subangular, oolitic sand is medium- to coarse-grained, ooid sand grains are rounded to subrounded; gravel is rounded to subrounded and locally derived, pebble to boulder size, and carbonate clasts are subrounded to angular and 1 to 6 inches (3–15 cm) in diameter and 1 to 2 inches (3–5 cm) thick; thin to medium bedded; sand grains are 25% to 75% ooids with varying amounts of quartz, lithic fragments, carbonate pebbles, and mica flakes; ooids formed in Great Salt Lake and were transported onto Antelope Island beach deposits by wave action; carbonate chips and pebbles appear to be rip-up clasts of cemented ooids and/or laminated algal mats that have washed up on the shore; mapped on the beaches and spits of Antelope Island; interbedded with or laterally gradational with playa mud deposits (Qlpm) and oolitic sand deposits (Qlos); thickness 1 to 10 feet (0.3–3 m).

Qlgb **Lacustrine gravel and sand related to Bonneville shoreline and transgressive phase of Lake Bonneville** (upper Pleistocene) – Moderately to well-sorted gravel and sand, and minor silt, and boulders; clasts are typically well rounded and sorted (Clark and others, 2017); thin to thick bedded; mapped as veneers over bedrock; only mapped between the Bonneville and Provo shorelines on Antelope Island; thickness variable, 0 to 100 feet (0–30 m).

Qll **Lagoon-fill deposits** (Holocene) – Moderately sorted, yellowish-gray silt and clay with sand and gravel; quartz sand is fine to coarse grained and subangular to angular, contains ooids deposited from Great Salt Lake during high water years, where present the ooids comprise up to 25% of the unit; subrounded to rounded pebble gravel common near spit gravel bars; mapped behind Holocene spits on the south side of Antelope Island; estimated thickness less than 10 feet (3 m).

Qlos **Lacustrine oolitic sand deposits** (Holocene) – Moderately to well-sorted, light olive-gray to yellowish-gray oolitic sand, carbonate chips and clasts, and minor silt; oolitic sand is medium to coarse grained; quartz and lithic sand grains are angular to subangular and ooid sand grains are rounded to subrounded; carbonate chips and clasts are subrounded to angular; thin to medium bedded; sand grains vary from 10% to 75% ooids (with higher concentrations near the Great Salt Lake beach ridge crest), with varying amounts of quartz, lithic fragments, carbonate fragments, and mica flakes; carbonate chips and clasts are 0.5 to 6 inches (1–15 cm) in diameter and 1 to 2 inches (3–5 cm) thick; ooids formed in Great Salt Lake and were deposited on delta barrier bars and islands by wave action; carbonate chips and clasts, commonly flat in shape, appear to be rip-up clasts of cemented ooids and/or laminated algal mats or microbialite carbonates (Qlmk) that have washed up on the shore; mapped on the delta front of the lobate paleodelta (Qdy) that formed at the mouth of the paleo-Jordan River meander channel near Browns Island (plate 2), extends eastward and southwest on small islands and barrier bars near the Great Salt Lake shoreline; mapped on surfaces that are elevated above young lacustrine mud deposits (Qlmy) and younger deltaic deposits (Qdy); interbedded with or laterally gradational with playa mud deposits (Qlpm) and lacustrine sand and gravel (Qlgy); typically overlies lacustrine silt and clay deposits; thickness 1 to 6 feet (0.3–2 m).

Four samples were collected from the lobate delta beach ridge crest or barrier bar of unit Qlos (table 2; Antelope Island South quadrangle). Three ooid samples were collected from two distinct layers separated by an A-horizon soil that developed on the lower deposit (figure 3), and a bulk soil sample was also collected from the soil (McKean and others, 2016). The ooid cortex and core radiocarbon ages from the upper and lower deposits show formation between 6000 and 7500 cal yr B.P. (calibrated radiocarbon age range rounded to nearest 500 years from McKean and others, 2016). We also used radiocarbon to date the organic material in the soil developed on the lower ooid deposit and it had an average calibrated age of 344 ± 15 cal yr B.P. (McKean and others, 2016). Ooids formed in Great Salt Lake between 6000 and 7500 years ago were transported along the shore and deposited on the paleo-Jordan River lobate delta barrier bar. The young soil probably developed during a period of low Great Salt Lake levels, followed by lake level rise and deposition of a second barrier bar ooid deposit over the first (figure 3), but the young soil age could also be interpreted as contamination of the bulk sample by modern rootlets (McKean and others, 2016).

Qlpm **Lacustrine and playa mud deposits** (Holocene) – Moderately to poorly sorted, light olive-gray silt and clay with oolitic sand; sand is fine to coarse grained and interlayered with the clay and silt, but also forms thin discontinuous sand lenses; sand makes up approximately 25% to 50% of the playa mud deposit; locally the mud and sand are underlain by an olive-gray to olive-black clay and silt, and in places by Lake Bonneville clay, marl, and sand with ostracodes; quartz and lithic sand grains are angular to subangular and ooid sand grains are rounded to subrounded; thin to medium bedded; sand grains vary from approximately 25% to 75% ooids, and variable quartz, lithic fragments, and mica flakes; locally includes halite, gypsum, and other salts that form thin deposits on the playa surface; located along the shore of Great Salt Lake where ooids are potentially forming in situ during high water or being brought into the beach and shoreface by wave action; locally contains carbonate chips and clasts; interbedded with or laterally gradational with young lacustrine mud deposits (Qlmy), oolitic sand deposits (Qlos), and lacustrine sand and gravel (Qlgy); in some locations fins and ridges of desiccated and eroded carbonate microbialite mounds are contained in the playa mud (see unit Qlmk); mapped as unit Qli by Sack (2005) in the Clearfield quadrangle; exposed thickness of 0 to 3 feet (0–1 m).

Qlmy **Young lacustrine mud deposits** (Holocene to upper Pleistocene?) – Moderately to well-sorted, yellowish-brown to olive-gray silt, clay, and minor sand; sand is fine to medium grained; silt is unbedded with thin discontinuous stringers of clay and sand; clay is light olive-gray to olive-gray marl and is locally mottled; the sand is olive gray to moderate brown and composed of subangular to angular grains of quartz, lithic fragments, and mica flakes, and locally ooids; locally includes halite, gypsum, and other salts that form thin deposits on the ground surface; mapped on mud flats between lacustrine and deltaic sediments (Qly, Qldy), conceals deltaic distributary channels in the lobate delta (Browns Island) area; mapped on lightly to non-vegetated mud flats that are flooded periodically by Great Salt Lake, shallow groundwater, or occasionally by water-control structures that flood these lowlands for wetlands mitigation or ponding for duck clubs and bird refuges; distinguished on aerial photographs from Qly by the characteristic, low-lying, white mud flats and lack of vegetation; includes mud flats from Holocene highstands above the historical high of Great Salt Lake; interbedded with or laterally gradational with playa mud deposits (Qlpm); unit may include Gilbert or regressive Bonneville clays where the Gilbert tufa is absent; in places the unit forms a thin veneer over the underlying Gilbert-age tufa breccia (tufa found in the

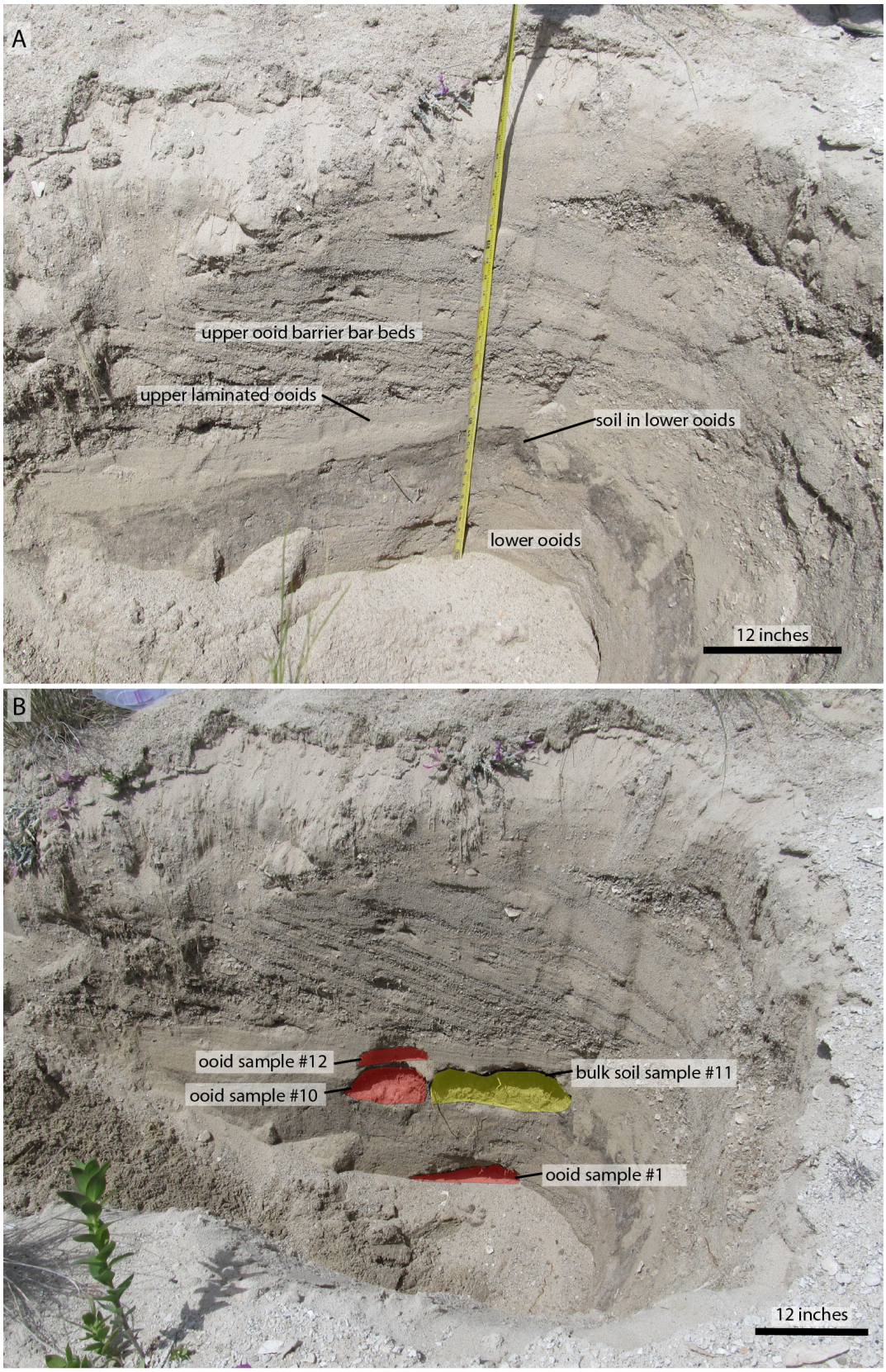


Figure 3. *North view of the sample trench located within the lobate delta barrier bar of the Antelope Island South and Baileys Lake quadrangles. (A) The lower ooids are darker gray than the upper ooids and have a soil developed on the upper surface; the upper ooids overlie the soil in fine-grained laminate deposition, followed by higher angle beds that are coarser grained with angular to rounded carbonate grains (both spherical and flat in nature). Tape measure in inches/feet for scale. (B) Approximately same view as A. The red highlighted areas represent the ooid samples and the yellow highlighted area represents the bulk soil sample for radiocarbon dating (see table 2, and McKean and others, 2016).*

subsurface as a cemented layer or broken pebble-size clasts) and clay, and Bonneville age olive-gray and red-brown clay and olive-gray quartz sands (see figure 4) (Hylland and others, 2012, 2014); unit correlative with lacustrine mud deposits mapped as Qlmy in the Magna quadrangle by Solomon and others (2007, 2018); estimated less than 10 feet (3 m) thick.

Qlmk **Lacustrine mud and microbial carbonates** (Holocene?) – Desiccated and eroded carbonate microbialite mounds within the playa mud and oolitic sands (figure 5); fins and ridges of wavy elongate ovals with single and double ridges that are aligned to the northwest; some ovals are larger than 3 feet (1 m) in length (see figure 5), individual pieces of carbonate ridges are 6 to 12 inches (15–30 cm) long, 4 to 8 inches (10–20 cm) tall, and 1 to 3 inches (2–7 cm) wide; one deposit mapped along the southeast shore of Great Salt Lake; erosion has removed the upper surface and inner parts of the mounds; similar to microbial mounds, ridges (on polygonal desiccation ridges), and mats present in other areas around Great Salt Lake (see Vanden Berg and others, 2015, 2016; Frantz and others, 2017; Janecke and Evans, 2017); other unmapped microbial deposits may exist in the playa mud deposits (Qlpm) or below the historical average Great Salt Lake water-level elevation; carbonate ridges about 1 foot (~0.3 m) thick, exposed mud deposits 0 to 3 feet (0–1 m) thick.

Qly **Young lacustrine deposits** (Holocene to upper Pleistocene?) – Moderately sorted silt, sand, clay, and marl; dark yellowish-brown silt, olive-gray quartz sand, light olive-gray clay, and yellowish-gray marl; quartz sand is fine to coarse grained and subangular to angular; sand locally contains ooids (5% to 15%); mapped where lacustrine sediments form low "islands" or elevated mounds, surrounded by or including young lacustrine mud deposits (Qlmy) and spring and marsh deposits (Qsm); distinguished from Qlmy by the presence of vegetation, the lack of mud flats, and an elevated island-like geomorphology; distinguished from younger deltaic (Qdy) and lacustrine and deltaic (Qldy) deposits by the lack of natural levee deposits and deltaic distributary channels; as mapped, unit may include or be underlain by



Figure 4. *View to northeast of Bonneville and post-Bonneville deposits exposed in the canal cut of the Goggin Drain, Baileys Lake quadrangle. Units from top to bottom are: (A) upper light gray fine sand and clay that may be post-Bonneville Gilbert-episode and/or Great Salt Lake sediments, (B) slope-forming light olive-gray regressive Lake Bonneville clay and silt, and (C) transgressive Lake Bonneville red-brown clay and marl. No direct ages have been determined for this site, but units are probably lithologically correlative with deposits exposed at the Baileys Lake paleoseismic trench site where Gilbert-episode deposit OSL samples yielded 11.5 ± 5.2 ka and 12.5 ± 1.8 ka; regressive-phase deposits ranged from 13.1 ± 1.2 ka and 14.1 ± 1.6 ka; and transgressive-phase deposits ranged from 19.3 ± 0.8 ka to 31.6 ± 3.3 ka (Hylland and others, 2012, 2014). Exposed bank is 5 to 7 feet (1.5–2 m) tall. Photograph location 40.816660° N, 112.101024° W, NAD83.*



Figure 5. *View to northwest of the southeastern shore of Great Salt Lake showing fins and ridges of desiccated and eroded carbonate microbialite mounds that are contained within the playa mud (*Qlmk*). The wavy carbonate ridges form ovals (single and double walled) that align to the northwest; erosion has removed the upper surface and inner parts of the mounds. Photograph from Antelope Island South quadrangle, approximate location 40.8081° N, 112.1395° W, NAD83.*

Gilbert-age tufa breccia (tufa found in the subsurface as a cemented layer or broken pebble-size clasts) and clays, and Bonneville-age olive-gray and red-brown clays and olive-gray quartz sands (Hylland and others, 2012, 2014); the lacustrine deposits have erosional and depositional Great Salt Lake shorelines on the islands; locally includes a loess veneer and buried soil; unit correlative with young lacustrine deposits mapped as Qly in the Magna quadrangle by Solomon and others (2007, 2018); exposed thickness less than 6 feet (2 m).

Spring and Marsh Deposits

Qsm **Spring and marsh deposits** (Holocene) – Silt, clay, and organic-rich sediment associated with springs, ponds, seeps, and wetlands; commonly wet, but seasonally dry; may locally contain peat deposits; overlies young lacustrine deposits (Qly); mapped where the water table is high: supports the growth of tall reeds which aid mapping on aerial photographs; some marsh deposits are the result of impounded water and wetlands controlled by dikes and water-control actions of the duck clubs, for wetlands mitigation, and for migratory bird refuges; some smaller spring and marsh deposits are not mapped because they are too small to show separately at map scale; estimated thickness less than 6 feet (2 m).

Mixed-Environment Deposits

Qldy **Young lacustrine and deltaic deposits** (Holocene to upper Pleistocene?) – Well to moderately sorted, light olive-gray to moderate yellowish-brown, silty sand, clay, and marl; commonly more clay rich with very little silt and sand; contains thin to medium-bedded discontinuous sand, clay, and silt lenses; sand is fine to medium grained, subangular to rounded; sand grains include quartz, lithic fragments, and mica flakes; distinguished from younger deltaic deposits (Qdy) by its broad, uniformly flat geomorphic surface along the paleo-Jordan River channels and deltas, and from young lacustrine deposits (Qly) by the presence of alluvial channels, deltaic distributary channels, and deltaic fan deposits overlying and incised into the deposit; locally includes an upper and lower surficial loess veneer separated by a buried soil; correlates with both young lacustrine deposits (Qly) and young deltaic deposits (Qldy) as mapped by Solomon and others (2007, 2018) in the northern part of the Magna quadrangle, as well as deltaic deposit units mapped as units ldc, ldm, fm, fdf, fdc, fdco, and fdcy by Van Horn (1979, 1982) in the Salt Lake City South and North quadrangles; may include Gilbert-age tufa breccia (tufa found in the subsurface as a cemented layer or broken up pebble-size clast) and clays, and Bonneville age olive-gray and red-brown clay and marl and olive-gray quartz sands (Hylland and others, 2012, 2014); Hylland and others' (2012, 2014) paleoseismic trench (in this unit) yielded ages for the surficial loess and underlying Gilbert, Bonneville, and pre-Bonneville deposits: optically stimulated luminescence (OSL) dating yielded ages of 3.2 ± 0.5 ka and 12.5 ± 1.4 ka for upper and lower loess deposits, respectively, 11.5 ± 5.2 ka and 12.5 ± 1.8 ka for Gilbert-episode deposits, 13.0 ± 1.2 ka to 14.1 ± 1.6 ka for regressive phase deposits, and 19.3 ± 0.8 ka to 31.6 ± 3.3 ka for transgressive phase deposits, and radiocarbon dating yielded an age of 35.8 ± 0.8 cal ka for pre-Bonneville deposits; exposed thickness less than 10 feet (3 m).

Stacked-Unit Deposits

Qh/Tsl **Human disturbance over Salt Lake Formation, undivided** (historical over Pliocene? to Miocene) – One area of deposits and disturbed ground from aggregate

quarrying at a large gravel pit on the southeast side of Antelope Island; quarrying mostly removed gravel and sand deposited by Lake Bonneville exposing Neogene Salt Lake Formation; only mapped on Antelope Island near the northern border of the Antelope Island South quadrangle; thickness variable.

Qsm/Qaly

Spring and marsh deposits over young stream deposits, undivided (Holocene) – A veneer of spring and marsh deposits partly conceal young stream deposits; mapped where marsh reeds and wetlands fill the lowlands created by the paleo-Jordan River channel near the Baileys Lake area (plate 2); some marsh deposits may be the result of impounded water and wetlands controlled by dikes and water-control actions for wetlands mitigation and migratory bird refuges; smaller spring and marsh deposits are not mapped because they are too small to show separately at map scale; estimated thickness of Qsm less than 6 feet (2 m) and the exposed thickness of Qaly is less than 15 feet (5 m).

Unconformity

TERTIARY (NEOGENE)

Tsl **Salt Lake Formation, undivided** (Pliocene? to Miocene) – Only mapped as a stacked unit (Qh/Tsl), gray to light gray tuffaceous sandstone, conglomerate, volcanic ash, marl, and mudstone (unit description modified from Doelling and others, 1990, 2018; Willis and Jensen, 2000; Willis and others, 2010; and Clark and others, 2017); tuffaceous sandstone is very fine grained, moderately indurated, laminated to medium bedded, locally cross-bedded, noncalcareous, and porous; conglomerate is crudely stratified with clasts of quartzite and limestone cobbles that are subangular to subrounded in a calcareous sandy matrix; volcanic ash consisting of glass shards (up to 100% angular volcanic glass) is present within poorly exposed fine-grained sediments; only a small exposure (Qh/Tsl) is within the Antelope Island South quadrangle near the northern boundary, the unit is more widely exposed to the north on the eastern side of Antelope Island in small outcrops, float, and within a now-reclaimed sand and gravel pit; tephrochronology from tuffs on the east side of Antelope Island indicate ages from 11 to 8 Ma (Willis and Jensen, 2000), Bryant and others (1989) reported a fission track age on zircon of 6.1 ± 1.1 Ma; based on nearby samples with ages of 11 to 8 Ma, Willis and Jensen (2000) suggested that the Bryant and others (1989) ages may err on the young side; see Clark and others (2017) for regional ages of Tsl; assuming no structural complexities and a uniform strike and dip thickness on Antelope Island, unit Tsl is at least 1800 feet (550+ m) thick.

Major unconformity

CRETACEOUS TO PALEOPROTEROZOIC

Farmington Canyon Complex – In the Wasatch Range, Bryant (1988) divided the Farmington Canyon Complex into four main units: (1) quartz-monzonite gneiss, (2) migmatite, (3) schist and gneiss, and (4) quartzite, gneiss, and schist. Yonkee and Lowe (2004) divided the complex into nine mappable units. Correlation with units between the Wasatch Range and Antelope Island is unclear (see Bryant, 1988; Yonkee and Lowe, 2004; Coogan and King, 2016; and Clark and others, 2017). On Antelope Island Doelling and others (1990, 2018) mapped 11 units, Yonkee and others (2000a) revised this to 10 units. Willis and others (2010) also revised some units and mapping of Antelope Island. Using Yonkee and others' (2000a) revised subdivision of the Paleoproterozoic Farmington Canyon Complex, seven units are mapped on the Antelope Island South quadrangle: (1) layered gneiss (Xfcl), (2) quartz-rich gneiss (Xfcq), (3) metamorphosed ultramafic rock (Xfcu), (4) banded gneiss (Xfcb), (5) granite and pegmatite (Xfcp), (6) chloritic gneiss, and (7) phyllonite and mylonite. Farmington Canyon Complex units previously mapped by Doelling and others (1990, 2018) as chloritized gneiss, mylonite, and phyllonite and by Yonkee (1992) and Yonkee and others (2000a) as chloritic gneiss and phyllonite, and mylonite, have experienced Cretaceous retrograde metamorphism and deformation and are here combined and mapped as altered and deformed rocks (KXa) after Coogan and King (2016) and Clark and others (2017). The Farmington Canyon Complex is Paleoproterozoic based on geochronologic data in nearby areas; Barnett and others (1993) reported $^{207}Pb/^{206}Pb$ monazite ages from gneisses that range from 1640 to 1720 Ma; Nelson and others (2002, 2011) reported a mean monazite microprobe age of 1705 ± 90 Ma from a gneiss; Mueller and others (2011) reported a $^{207}Pb/^{206}Pb$ age of 2450 Ma for inherited zircon in the granitic gneiss body and a ~1700 Ma $^{207}Pb/^{206}Pb$ age for metamorphic zircon overgrowths (table 6; Nelson and others, 2011; Mueller and others, 2011). $^{40}Ar/^{39}Ar$ ages of syn-deformational sericite found in ductile deformation zones are mostly between 110 and 140 Ma (Yonkee, 1990) and record the Cretaceous retrograde metamorphism and deformation that overprinted earlier structures (Yonkee, 1990; Yonkee and others, 2000a), see unit KXa.

Xfc **Farmington Canyon Complex, undivided** (Paleoproterozoic) – Undivided metamorphic and altered and deformed rocks (KXa), only shown on cross sections.

KXa **Altered and deformed rocks** (Cretaceous, Paleoproterozoic) – Altered and deformed rocks of the Farmington Canyon Complex, altered to dark-green to greenish-black chloritic and dark-reddish-brown

Table 6. *Summary of SHRIMP U-Pb zircon age analysis from the Antelope Island South quadrangle.*

Map No.	Sample No.	Map Unit	Rock Name	7.5' Quadrangle	Latitude (°N)	Longitude (°W)	Age (Ma)	Laboratory	Analysis Type	Reference
ZR1	01FCC8	Xfcl	biotite orthogneiss	Antelope Island South	40.856171	112.1759	1691 ± 26	ANU	Crystallization age	Nelson and others, 2011

Notes:
Map number corresponds to sample identification on Antelope Island quadrangle
Location given in table is approximate; based on NAD83; original location 0400950E 4523250N UTM NAD27 zone 12
Laboratory: ANU is Australian National University, Canberra, Australia

hematized gneiss, phyllonite and mylonite (unit description modified from Doelling and others, 1990, 2018; Yonkee and others, 2000a; Willis and others, 2010; and Clark and others, 2017); locally cut by quartz veins and silicic alteration; chloritic gneiss grades into phyllonite and mylonite; original minerals within the chloritic gneiss are altered to sericite, fine-grained chlorite, biotite, stilpnomelane, epidote, and albite; phyllonite and mylonite shear zones are composed of sericite, chlorite, quartz, and feldspar; only mapped on Antelope Island, but may represent some of the metamorphic basement rocks encountered in drill holes (e.g., Arnow and Mattick, 1968; Willis and Jensen, 2000); previously mapped by Doelling and others (1990, 2018) as chloritized gneiss, mylonite, and phyllonite (units XWfg and XWfs) and by Yonkee and others (2000a) as chloritic gneiss and phyllonite, and mylonite; retrograde metamorphism and deformation of older Farmington Canyon Complex rocks likely occurred during the Cretaceous Sevier orogeny (Yonkee, 1990; Yonkee and others, 2000a), the rocks are here mapped as unit KXa after Clark and others (2017).

Xfcp **Granite and pegmatite** (Paleoproterozoic) – Small knobby plutons of red granite are mapped on the Antelope Island South quadrangle; map unit description includes units to the north on the rest of Antelope Island; white to light gray and pink, weakly to nonfoliated, coarse-grained granite and pegmatite (unit description modified from Doelling and others, 1990, 2018; Yonkee and others, 2000a; Willis and others, 2010; and Clark and others, 2017); includes pegmatitic granite on the eastern part of the island, garnet-muscovite-bearing granite that forms small pods, red granite that forms small plutons on the southern part of the island, and pegmatite that forms dikes and pods; granite and pegmatite samples contain quartz (25%–40%), plagioclase (20%–35%), and potassium feldspar (30%–50%), with minor muscovite, garnet, biotite, and accessory minerals; unit is compositionally granite based on mineral modes; grain sizes vary from <1 to 10 mm in granite and locally >1 cm in pegmatite; weakly to nonfoliated; intrusive cross-cutting relationships indicate the granite and pegmatite unit is younger than most Farmington Canyon Complex units; dike emplacement occurred after most metamorphism; variable origins including partial melting of layered gneiss and late-stage intrusion into the Farmington Canyon Complex.

Xfcb **Banded gneiss** (Paleoproterozoic) – Light- to pinkish-gray, locally migmatitic gneiss with well-developed layering and foliation; hornblende-bearing, quartz-feldspar gneiss with lenses of hornblende-plagioclase gneiss and intruded by pegmatitic granite (unit description modified from Doelling and

others, 1990, 2018; Yonkee and others, 2000a; Willis and others, 2010; and Clark and others, 2017); contains quartz (30%–35%), plagioclase (25%–40%), potassium feldspar (15%–30%), hornblende (5%–10%), biotite (5%–10%), possible pyroxene, and accessory minerals including zircon, allanite, and apatite; unit is granitic to granodioritic in composition based on mineral modes; gneiss and granite are generally resistant and form ridges; mapped near the northern boundary of the Antelope Island South quadrangle; contacts are gradational or interlayered; gneiss probably represents margin of a Paleoproterozoic granite intrusion that occurred prior to or synchronous with metamorphism.

Xfcu **Metamorphosed ultramafic rock** (Paleoproterozoic) – Dark-green to black, metamorphosed ultramafic rocks consisting of amphibole, pyroxene, and rare olivine that are variably altered to chlorite, serpentine, and talc (unit description modified from Doelling and others, 1990, 2018; Yonkee and others, 2000a; Willis and others, 2010; and Clark and others, 2017); contains amphibole (15%–30%), pyroxene (10%–15%), olivine (0%–10%), alteration minerals, and accessory minerals; commonly forms dike- and sill-like masses within layered gneiss; mapped at two outcrops on the southeast side of Antelope Island; weak to well-developed foliation, widespread alteration to serpentine; may represent parts of Paleoproterozoic ultramafic lava flows, layered mafic complex, or oceanic crust.

Xfcq **Quartz-rich gneiss** (Paleoproterozoic) – White to light-gray quartz-plagioclase gneiss with minor layered gneiss and biotite schist; weathers to vitreous, milky to greenish-gray (unit description modified from Doelling and others, 1990, 2018; Yonkee and others, 2000a; Willis and others, 2010; and Clark and others, 2017); consists of quartz (80%–95%), plagioclase (5%–10%), biotite (0%–5%), muscovite (0%–5%), and accessory minerals including magnetite, zircon, and hematite; forms resistant ridges of concordant lenses ranging from 3 to 100 feet (1–30 m) wide within the layered gneiss (Xfcl); foliation defines preferred orientation of mica, and quartz is recrystallized; probably metamorphosed Paleoproterozoic quartz-rich sedimentary protolith.

Xfcl **Layered gneiss** (Paleoproterozoic) – Light- to dark-gray to brown to pink layered gneiss, migmatitic with well-developed compositional layering of quartzofeldspathic, biotite-rich, quartz-rich, amphibolite layers from 0.2 to 6 feet (0.05–2 m) thick (unit description modified from Doelling and others, 1990, 2018; Yonkee and others, 2000a; Willis and others, 2010; and Clark and others, 2017); contains widespread pegmatitic dikes, lenses of biotite schist and quartz-rich gneiss and rare pods of metamorphosed ultramafic and mafic rock; grades locally to biotite schist and quartz-rich gneiss; mineral abundances of layered gneiss consist of variable amounts of quartz (20%–45%), plagioclase (25%–45%), potassium feldspar (5%–15%), biotite (5%–30%), garnet (0%–10%), and rare sillimanite and cordierite, accessory minerals include zircon, allanite, and apatite; weathers to brown slopes and subdued ledges; well-developed foliation and compositional layering, isoclinal folds, migmatitic texture; U-Pb zircon age of 1691 ± 26 Ma from layered gneiss on southern Antelope Island (Nelson and others, 2011) (table 6, sample 01FCC8; Antelope Island quadrangle, map number ZR1); probably metamorphosed Paleoproterozoic graywacke and feldspathic sandstone protolith (Willis and others, 2010).

ACKNOWLEDGMENTS

The geologic map of the Baileys Lake quadrangle was funded by the Utah Geological Survey and the U.S. Geological Survey, National Cooperative Geologic Mapping Program, through USGS STATEMAP award number G12AC20226. The geologic maps of the Antelope Island South and Saltair NE quadrangles were funded by the Utah Geological Survey.

Discussions with Jon K. King, Christian Hardwick, Don Clark, Doug Sprinkel (all UGS), and Jack Oviatt (Kansas State University, retired) helped improve these maps and report. UGS staff members Jessica Castleton, Ben Erickson, and Adam Hiscock assisted with fieldwork. Stefan Kirby, Don Clark, Grant Willis, and Stephanie Carney improved these maps and associated materials through their reviews. Kent Brown (UGS) assisted with setting up the digital photogrammetry. Kent Brown and Jay Hill (UGS) and Corey Unger (formerly UGS) provided technical advice and assistance with the map and figures. Basia Matyjasik and Don Clark (UGS) and David Dinter (University of Utah) provided their compiled GIS data for Antelope Island and the Great Salt Lake fault zone. We are grateful to all the private property owners who allowed us access to their property for field mapping purposes.

REFERENCES

Arnow, T., and Mattick, R.E., 1968, Thickness of valley fill in the Jordan Valley east of the Great Salt Lake, Utah, *in* Geological Survey Research, 1968: U.S. Geological Survey Professional Paper 600–B, p. B79–82.

Arnow, T., and Stephens, D., 1990, Hydrologic characteristics of the Great Salt Lake, Utah—1847–1986: U.S. Geological Survey Water-Supply Paper 2332, 32 p., map scale 1:125,000.

Atwood, G., 2006, Shoreline superelevation—evidence of coastal processes of Great Salt Lake, Utah: Utah Geological Survey Miscellaneous Publication 06–9, 231 p.

Atwood, G., and Mabey, D.R., 1995, Flooding hazards associated with Great Salt Lake, *in* Lund, W.R., editor, Environmental and engineering geology of the Wasatch Front region: Utah Geological Association Publication 24, p. 483–494.

Barnett, D., Bowman, J.R., and Smith, H.A., 1993, Petrologic and geochronologic studies in the Farmington Canyon Complex, Wasatch Mountains and Antelope Island, Utah: Utah Geological Survey Contract Report 93–5, 35 p.

Baskin, R.L., and Allen, D.V., 2005, Bathymetric map of the south part of Great Salt Lake, Utah, 2005: U.S. Geological Survey Scientific Investigations Map 2894.

Baskin, R.L., and Turner, J., 2006, Bathymetric map of the north part of Great Salt Lake, Utah, 2006: U.S. Geological Survey Scientific Investigations Map 2954.

Biek, R.F., Solomon, B.J., Keith, J.D., and Smith, T.W., 2005, Geologic map of the Tickville Spring quadrangle, Salt Lake and Utah Counties, Utah: Utah Geological Survey Map 214, 2 plates, scale 1:24,000.

Biek, R.F., Solomon, B.J., Smith, T.W., and Keith, J.D., 2007, Geologic map of the Copperton quadrangle, Salt Lake County, Utah: Utah Geological Survey Map 219, 2 plates, scale 1:24,000.

Biek, R.F., Solomon, B.J., Smith, T.W., and Keith, J.D., 2018, Geologic map of the Copperton quadrangle, Salt Lake County, Utah (GIS reproduction of 2007 map): Utah Geological Survey Map 219DM, 2 plates, scale 1:24,000.

Bortz, L.C., 2002, Heavy-oil deposit, Great Salt Lake, Utah, *in* Gwynn, J.W., editor, Great Salt Lake, an overview of change: Utah Geological Survey and Department of Natural Resources Special Publication, p. 243–250.

Bortz, L.C., Cook, S.A., and Morrison, O.J., 1985, Great Salt Lake area in Utah, *in* Gries, R.R., and Dyer, R.C., editors, Seismic exploration of the rocky mountain region: The Rocky Mountain Association of Geologists and the Denver Geophysical Society, Denver, Colorado, p. 275–281.

Bowman, S.D., and Lund, W.R., editors, 2016, Guidelines for investigating geologic hazards and preparing engineering-geology reports, with a suggested approach to geologic-hazard ordinances in Utah: Utah Geological Survey Circular 122, 156 p., 4 appendices.

Bronk Ramsey, C., 2009, Bayesian analysis of radiocarbon dates: Radiocarbon, v. 51, no. 1, p. 337–360.

Bryant, B., 1988, Geology of the Farmington Canyon Complex, Wasatch Mountains, Utah: U.S. Geological Survey Professional Paper 1476, 54 p., 1 plate, scale 1:50,000.

Bryant, B., 1990, Geologic map of the Salt Lake City 30′ x 60′ quadrangle, north-central Utah, and Uinta County, Wyoming: U.S. Geological Survey Miscellaneous Investigations Series Map I–1944, 2 plates, scale 1:100,000.

Bryant, B., Naeser, C.W., Marvin, R.F., and Mehnert, H.H., 1989, Ages of late Paleogene and Neogene tuffs and the beginning of rapid regional extension, eastern boundary of the Basin and Range Province near Salt Lake City, Utah: U.S. Geological Survey Bulletin 1787–K, 11 p.

Clark, D.L., Oviatt, C.G., and Dinter, D.A., 2017, Interim geologic map of the Tooele 30′ x 60′ quadrangle, Tooele, Salt Lake, and Davis Counties, Utah: Utah Geological Survey Open-File Report 669DM, 43 p., 3 plates, scale 1:62,500.

Clark, D.L., Oviatt, C.G., and Dinter, D.A., in review, Geologic map of the Tooele 30′ x 60′ quadrangle, Tooele, Salt Lake, and Davis Counties, Utah: Utah Geological Survey Map, scale 1:62,500.

Colman, S.M., Kelts, K.R., and Dinter, D.A., 2002, Depositional history and neotectonics in Great Salt Lake, Utah, from high-resolution seismic stratigraphy: Sedimentary Geology, v. 148, p. 61–78.

Coogan, J.C., and King, J.K., 2016, Interim geologic map of the Ogden 30′ x 60′ quadrangle, Box Elder, Cache, Davis, Morgan, Rich, and Summit Counties, Utah, and Uinta County, Wyoming: Utah Geological Survey Open-File Report 653DM, 147 p., 3 plates, scale 1:62,500.

Cook, K.L., and Berg, J.W., 1961, Regional gravity survey along the central and southern Wasatch Front, Utah: U.S. Geological Survey Professional Paper 316–E, plate 13, p. 75–89.

Currey, D.R., and James, S.R., 1982, Paleoenvironments of the northeastern Great Basin and northeastern Basin Rim region—a review of geological and biological evidence, *in* Madsen, D.B., and O'Connell, J.F., editors, Man and environment in the Great Basin: Society for American Archeology Papers, no. 2, p. 27–52.

Dinter, D.A., and Pechmann, J.C., undated, Paleoseismology of the East Great Salt Lake fault (Phase 3): Final Technical Report for U.S. Geological Survey, award number 00HQGR0099, 7 p.

Dinter, D.A., and Pechmann, J.C., 2005, Segmentation and Holocene displacement history of the Great Salt Lake fault, Utah, *in* Lund W.L., editor, Proceedings volume, Basin and Range Province Seismic Hazards Summit II: Utah Geological Survey Miscellaneous Publication 05–2, CD, 5 p. (extended abstract).

Dinter, D.A., and Pechmann, J.C., 2014, Paleoseismology of the Promontory segment, East Great Salt Lake fault: Final Technical Report for U.S. Geological Survey, award number 02HQGR0105, 23 p.

Doelling, H.H., and Willis, G.C., 1995, Guide to authors of geologic maps and text booklets of the Utah Geological Survey: Utah Geological Survey Circular 89, 98 p.

Doelling, H.H., Willis, G.C., Jensen, M.E., Hecker, S., Case, W.F., and Hand, J.S. (with contributions by Davis, F.D., Klauk, R.H., Gwynn, J.W., Bishop, C.E., and Atwood, G.), 1990, Geologic map of Antelope Island, Davis

County, Utah: Utah Geological Survey Map 127, 27 p., 2 plates, scale 1:24,000.

Doelling, H.H., Willis, G.C., Jensen, M.E., Hecker, S., Case, W.F., and Hand, J.S. (with contributions by Davis, F.D., Klauk, R.H., Gwynn, J.W., Bishop, C.E., and Atwood, G.), 2018, Geologic map of Antelope Island, Davis County, Utah (GIS reproduction of UGS Map 127 [1990]): Utah Geological Survey Map 127DR, 27 p., 2 plates, scale 1:24,000.

DuRoss, C.B., and Hylland, M.D., 2015, Synchronous ruptures along a major graben-forming fault system—Wasatch and West Valley fault zones, Utah: Bulletin of the Seismological Society of America, v. 105, no. 1, p. 14–37.

Duguid, S.M.A., Kyser, T.K., James, N.P., and Rankey, E.C., 2010, Microbes and ooids: Journal of Sedimentary Research, v. 80, p. 236–251.

Eardley, A.J., 1938, Sediments of Great Salt Lake, Utah: Bulletin of the American Association of Petroleum Geologists, v. 22, no. 10, p. 1305–1411.

Eardley, A.J., and Gvosdetsky, V., 1960, Analysis of Pleistocene core from Great Salt Lake, Utah: Geological Society of America Bulletin, v. 71, p. 1323–1344.

Eardley, A.J., Shuey, R.T., Gvosdetsky, V., Nash, W.P., Picard, M.D., Grey, D.C., and Kukla, G.J., 1973, Lake cycles in the Bonneville basin, Utah: Geological Society of America Bulletin, v. 84, p. 211–216.

Frantz, C., Matyjasik, M., Newell, D.L., Vanden Berg, M.D., and Park, C., 2017, Questioning the origin of the Great Salt Lake "microbialites" [abstract]: American Geophysical Union, fall meeting, paper EP12A–02, https://agu.confex.com/agu/fm17/meetingapp.cgi/Paper/292635.

Folk, R.L., 1993, SEM imaging of bacteria and nannobacteria in carbonate sediments and rocks: Journal of Sedimentary Petrology, v. 63, no. 5, p. 990–999.

Folk, R.L., and Lynch, L.F., 2001, Organic matter, putative nannobacteria and the formation of ooids and hardgrounds: Sedimentology, v. 48, no. 2, p. 215–229.

Godsey, H.S., Currey, D.R., and Chan, M.A., 2005, New evidence for an extended occupation of the Provo shoreline and implications for regional climate change, Pleistocene Lake Bonneville, Utah, USA: Quaternary Research, v. 63, p. 212–223.

Godsey, H.S., Oviatt, C.G., Miller, D.M., and Chan, M.A., 2011, Stratigraphy and chronology of offshore to nearshore deposits associated with the Provo shoreline, Pleistocene Lake Bonneville, Utah: Palaeogeography, Palaeoclimatology, Palaeoecology, v. 310, nos. 3–4, p. 442–450.

Graff, P.J., Sears, J.W., and Holden, G.S., 1980, The Uinta arch project—investigations of uranium potential in Precambrian X and older metasedimentary rocks in the Uinta and Wasatch Ranges, Utah and Colorado: U.S. Department of Energy Open-File Report GJBX–170(80), 180 p., 6 plates, map scale 1:48,000.

Halley, R.B., 1977, Ooid fabric and fracture in the Great Salt Lake and the geologic record: Journal of Sedimentary Petrology, v. 47, no. 3, p. 1099–1120.

Hedge, C.E., Stacey, J.S., and Bryant, B., 1983, Geochronology of the Farmington Canyon Complex, Wasatch Mountains, Utah: Geological Society of America Memoir 157, p. 37–44.

Hill, J., Benz, H., Murphy, M., and Schuster, G., 1990, Propagation and resonance of SH waves in the Salt Lake Valley, Utah: Bulletin of the Seismological Society of America, v. 80, no. 1, p. 23–42.

Hylland, M.D., DuRoss, C.B., McDonald, G.N., Olig, S.S., Oviatt, C.G., Mahan, S.A., Crone, A.J., and Personius, S.F., 2012, Basin-floor Lake Bonneville stratigraphic section as revealed in paleoseismic trenches at the Baileys Lake site, West Valley fault zone, Utah, *in* Hylland, M.D., and Harty, K.M., editors, Selected topics in engineering and environmental geology in Utah: Utah Geological Association Publication 41, p. 175–193.

Hylland, M.D., DuRoss, C.B., McDonald, G.N., Olig, S.S., Oviatt, C.G., Mahan, S.A., Crone, A.J., and Personius, S.F., 2014, Late Quaternary paleoseismology of the West Valley fault zone—insights from the Baileys Lake trench site, *in* DuRoss, C.B., and Hylland, M.D., Evaluating surface faulting chronologies of graben-bounding faults in Salt Lake Valley, Utah—new paleoseismic data from the Salt Lake City segment of the Wasatch fault zone and the West Valley fault zone—Paleoseismology of Utah, Volume 24: Utah Geological Survey Special Study 149, p. 41–76, 8 appendices, 1 plate.

Hylland, M.D., Hiscock, A.I., McDonald, G.N., 2017, Paleoseismic investigation of the Taylorsville fault, West Valley fault zone, Salt Lake County, Utah: unpublished Utah Geological Survey final technical report to the U.S. Geological Survey, National Earthquake Hazards Reduction Program, award no. G15AP00117, 41 p., 7 appendices, 2 plates.

Janecke, S.U., and Evans, J.P., 2017, Revised structure and correlation of the Great Salt Lake, North Promontory, Rozel and Hansel Valley fault zones revealed by the 2015–2016 low stand of Great Salt Lake, *in* Lund, W.R., Emerman, S.H., Wang, W., and Zanazzi, A., editors, Geology and resources of the Wasatch—back to front: Utah Geological Association Publication 46, p. 295–360, 10 appendices.

Kahle, C. F., 1974, Ooids from Great Salt Lake, Utah, as an analogue for the genesis and diagenesis of ooids in marine limestones: Journal of Sedimentary Petrology, v. 44, no. 1, p. 30–39.

Keaton, J.R., and Currey, D.R., 1989, Earthquake hazard evaluation of the West Valley fault zone in the Salt Lake City urban area, Utah: Salt Lake City, Dames & Moore, unpublished technical report prepared for U.S. Geological Survey, contract no. 14–08–0001–G1397, 69 p. (Sub-

sequently published in 1993 as Utah Geological Survey Contract Report 93–7.)

Keaton, J.R., Currey, D.R., and Olig, S.J., 1987, Paleoseismicity and earthquake hazards evaluation of the West Valley fault zone, Salt Lake City urban area, Utah: Salt Lake City, Dames & Moore and University of Utah Department of Geography, unpublished technical report prepared for U.S. Geological Survey, contract no. 14–08–0001–22048, 55 p. + 33 p. appendix. (Subsequently published in 1993 as Utah Geological Survey Contract Report 93–8.)

Lambert, P.M., and West, J.C., 1989, Continuous seismic-reflection survey of the Great Salt Lake, Utah—east of Antelope and Fremont Islands: U.S. Geological Survey Water-Resources Investigation 88–4157, 17 p., 1 plate.

Lanphere, M.A., Champion, D.E., Christiansen, R.L., Izett, G.A., and Obradovich, J.D., 2002, Revised ages for tuffs of the Yellowstone Plateau volcanic field—assignment of the Huckleberry Ridge Tuff to a new geomagnetic polarity event: Geological Society of America Bulletin, v. 114, no. 5, p. 559–568.

Larsen, W.N., 1957, Petrology and structure of Antelope Island, Davis County, Utah: Salt Lake City, University of Utah, Ph.D. dissertation, 142 p., map scale 1:24,000.

Lowe, M., Kirby, S.M., and Harty, K.M., 2018, Geologic map of the Farmington quadrangle, Salt Lake and Davis Counties, Utah: Utah Geological Survey Map 279DM, 2 plates, scale 1:24,000.

Marine, I.W., and Price, D., 1964, Geology and ground-water resources of the Jordan Valley, Utah: Utah Geological and Mineralogical Survey Water-Resources Bulletin 7, 67 p.

Marsell, R.E., and Threet, R.L., 1960, Geologic map of Salt Lake County, Utah, *in* Crawford, A.L., editor, 1964, Geology of Salt Lake County: Utah Geological and Mineralogical Survey Bulletin 69, 190 p., 1 plate, scale 1:63,360.

Mathew, A.A.L., 1930, Origin and growth of the Great Salt Lake oolites: The Journal of Geology, v. 38, no. 7, p. 633–642.

McGee, D., Quade, J., Edwards, R.L., Broecker, W.S., Cheng, H., Reiners, P.W., and Evenson, P., 2012, Lacustrine cave carbonates—novel archives of paleohydrologic change in the Bonneville Basin (Utah, USA): Earth and Planetary Science Letters, v. 351–352, p. 182–194.

McGuire, K.M., 2014, Comparative sedimentology of Lake Bonneville and the Great Salt Lake: Provo, Utah, Brigham Young University, M.S. thesis, 34 p.

McKean, A.P., 2014, Interim geologic map of the Salt Lake City North quadrangle, Salt Lake and Davis Counties, Utah: Unpublished Utah Geological Survey contract deliverable map prepared for U.S. Geological Survey, USGS STATEMAP award no. G135AC00169, 42 p., 1 plate, scale 1:24,000.

McKean, A.P., 2017, Interim geologic map of the Salt Lake City South quadrangle, Salt Lake County, Utah: Utah Geological Survey Open-File Report 676, 17 p., 1 plate, scale 1:24,000.

McKean, A.P., Rey, K.A., Tingey, D.G., and Hylland, M.D., 2016, Report of radiocarbon dating analyses, Antelope Island South quadrangle, Utah: Utah Geological Survey Open-File Report 659, 3 p., online, https://ugspub.nr.utah.gov/publications/open_file_reports/ofr-659.pdf.

McNeil, B.R., and Smith, R.B., 1992, Upper crustal structure of the northern Wasatch Front, Utah, from seismic reflection and gravity data: Utah Geological Survey Contract Report 92–7, 62 p., 6 plates.

Miller, D.M., 2016, The Provo shoreline of Lake Bonneville, *in* Oviatt, C.G., and Shroder, J.F., Jr., editors, Lake Bonneville—a scientific update: Amsterdam, Elsevier, Developments in Earth Surface Processes, v. 20, chapter 7, p. 127–144.

Miller, D.M., Oviatt, C.G., Dudash, S.L., and McGeehin, J.P., 2005, Late Holocene highstands of Great Salt Lake at Locomotive Springs, Utah: Geological Society of America Abstracts with Programs, v. 37, no. 7, p. 335.

Miller, R.D., 1980, Surficial geologic map along part of the Wasatch Front, Salt Lake Valley, Utah: U.S. Geological Survey Miscellaneous Field Studies Map MF–1198, 13 p., 2 plates, scale 1:100,000.

Mohapatra, G.K., 1996, Faulting and basin geometry beneath the Great Salt Lake—implications for basin evolution and Cenozoic extension: Tucson, University of Arizona, Ph.D dissertation, 159 p.

Mueller, P.A., Wooden, J.L., Mogk, D.W., and Foster, D.A., 2011, Paleoproterozoic evolution of the Farmington zone—implications for terrane accretion in southwestern Laurentia: Lithosphere, v. 3, no. 6, p. 401–408.

Murchison, S.B., 1989, Fluctuation history of Great Salt Lake, Utah, during the last 13,000 years: Salt Lake City, University of Utah, Ph.D. dissertation, 137 p.

Nelson, A.R., and Personius, S.F., 1993, Surficial geologic map of the Weber segment, Wasatch fault zone, Weber and Davis Counties, Utah: U.S. Geological Survey Miscellaneous Investigations Series Map I–2199, 22 p., 1 plate, scale 1:50,000.

Nelson, S.T., Harris, R.A., Dorais, M.J., Heizler, M., Constenius, K.N., and Barnett, D.E., 2002, Basement complexes in the Wasatch fault, Utah, provide new limits on crustal accretion: Geology, v. 30, no. 9, p. 831–834.

Nelson, S.T., Hart, G.L., and Frost, C.D., 2011, A reassessment of Mojavia and a new Cheyenne Belt alignment in the eastern Great Basin: Geosphere, v. 7, no. 2, p. 513–527.

OpenTopography, 2011, Utah Geological Survey, U.S. Environmental Protection Agency, and Utah Division of Emergency Management, Floodplain Management Pro-

gram acquired 1 meter LiDAR data: Online, http://opentopo.sdsc.edu/gridsphere/gridsphere?gs_action=lidarDataset&cid=geonlidarframeportlet&opentopoID=OTLAS.042013.26912.1.

Oviatt, C.G., 2014, The Gilbert episode in the Great Salt Lake basin, Utah: Utah Geological Survey Miscellaneous Publication 14–3, 20 p.

Oviatt, C.G., 2015, Chronology of Lake Bonneville, 30,000 to 10,000 yr B.P.: Quaternary Science Reviews, v. 110, p. 166–171, Appendix A supplementary data available online, http://dx.doi.org/10.1016/j.quascirev.2014.12.016.

Oviatt, C.G., Currey, D.R., and Miller, D.M., 1990, Age and paleoclimatic significance of the Stansbury shoreline of Lake Bonneville, northeastern Great Basin: Quaternary Research, v. 33, p. 291–305.

Oviatt, C.G., Miller, D.M., McGeehin, J.P., Zachary, C., and Mahan, S., 2005, The Younger Dryas phase of Great Salt Lake, Utah, USA: Palaeogeography, Palaeoclimatology, Palaeoecology, v. 219, no. 3–4, p. 263–284.

Paradis, O.P., Corsetti, F.A., Bardsley, A., Hammond, D.E., Xu, X., and Walker, J.C., 2017, Radial ooids from Great Salt Lake (Utah) as paleoenvironmental archives—insights from radiocarbon chronology and stable isotopes [abstract]: American Geophysical Union, fall meeting, paper EP12A–06, https://agu.confex.com/agu/fm17/meetingapp.cgi/Paper/291106.

Pechmann, J.C., and Dinter, D.A., undated, Paleoseismology of the East Great Salt Lake fault: Final Technical Report for U.S. Geological Survey, award number 98HQGR1013, variously paginated.

Pedone, V.A., and Norgauer, C.H., 2002, Petrology and geochemistry of recent ooids from the Great Salt Lake, Utah, *in* Gwynn, J.W., editor, Great Salt Lake—an overview of change: Special Publication of the Utah Department of Natural Resources, p. 33–41.

Personius, S.F., and Scott, W.E., 1992, Surficial geologic map of the Salt Lake City segment and parts of the adjacent segments of the Wasatch fault zone, Davis, Salt Lake, and Utah Counties, Utah: U.S. Geological Survey Miscellaneous Investigations Series Map I–2106, 1 plate, scale 1:50,000.

Petropoulous, G.S., 1994, Structure and relationships between Tertiary normal faults and Mesozoic thrust faults beneath the Great Salt Lake: Tucson, University of Arizona, M.S. thesis, 63 p., 6 plates.

Radkins, H., Murphy, M., and Schuster, G.T., 1989, Subsurface map and seismic risk analysis of the Salt Lake Valley: Utah Geological and Mineral Survey Open-File Report 152, 82 p., 4 plates.

Reimer, P.J., Bard, E., Bayliss, A., Beck, J.W., Blackwell, P.G., Bronk Ramsey, C., Buck, C.E., Cheng, H., Edwards, R.L., Friedrich, M., Grootes, P.M., Guilderson, T.P., Haflidason, H., Hajdas, I., Hatté, C., Heaton, T.J., Hoffmann, D.L., Hogg, A.G., Hughen, K.A., Kaiser, K.F., Kromer, B., Manning, S.W., Niu, M., Reimer, R.W., Richards, D.A., Scott, E.M., Southon, J.R., Staff, R.A., Turney, C.S.M., and van der Plicht, J., 2013, IntCal13 and Marine13 radiocarbon age calibration curves 0–50,000 years cal BP: Radiocarbon, v. 55, no. 4, p. 1869–1887.

Rey, K.A., 2012, Insights into the early transgressive history of Lake Bonneville from stratigraphic investigation of Pilot Valley, UT/NV, USA: Provo, Utah, Brigham Young University, M.S. thesis, 60 p.

Rio Tinto, undated, Tailings impoundment: Online, https://riotintokennecott.com/wp-content/uploads/2019/05/Tailings.pdf, accessed October 25, 2018.

Sack, D., 2005, Geologic map of the Clearfield 7.5′ quadrangle, Davis County, Utah: Utah Geological Survey Miscellaneous Publication 05–4, 14 p., 2 plates, scale 1:24,000.

Sandberg, P.A., 1975, New interpretations of Great Salt Lake ooids and of ancient non-skeletal carbonate mineralogy: Sedimentology, v. 22, p. 497–537.

Solomon, B.J., 1993, Quaternary geologic map of a portion of the Farnsworth Peak quadrangle, *in* Solomon, B.J., Quaternary geologic maps of Tooele Valley and the West Desert Hazardous Industry Area: Utah Geological Survey Open-File Report 296, 48 p., plate 13, scale 1:24,000.

Solomon, B.J., 1998, New evidence for the age of faulting on the West Valley fault zone: Utah Geological Survey, Survey Notes, v. 30, no. 3, p. 8 and 13.

Solomon, B.J., 2007, Surficial geologic map of part of the Kaysville quadrangle, Davis County, Utah: Utah Geological Survey Map 224, 2 plates, scale 1:24,000.

Solomon, B.J., Biek, R.F., and Smith, T.W., 2007, Geologic map of the Magna quadrangle, Salt Lake County, Utah: Utah Geological Survey Map 216, 2 plates, scale 1:24,000.

Solomon, B.J., Biek, R.F., and Smith, T.W., 2018, Geologic map of the Magna quadrangle, Salt Lake County, Utah (GIS reproduction of 2007 map): Utah Geological Survey Map 216DM, 2 plates, scale 1:24,000.

Tooker, E.W., and Roberts, R.J., 1971a, Geologic map of the Garfield [Farnsworth Peak] quadrangle, Salt Lake and Tooele Counties, Utah: U.S. Geological Survey Geologic Quadrangle Map GQ–922, 1 plate, scale 1:24,000.

Tooker, E.W., and Roberts, R.J., 1971b, Geologic map of the Magna quadrangle, Salt Lake County, Utah: U.S. Geological Survey Geologic Quadrangle Map GQ–923, 1 plate, scale 1:24,000.

Tooker, E.W., and Roberts, R.J., 1971c, Geologic map of the Mills Junction quadrangle, Tooele County, Utah: U.S. Geological Survey Geologic Quadrangle Map GQ–924, 1 plate, scale 1:24,000.

USDA Agricultural Stabilization and Conservation Service, 1937, Aerial photography, Project AAL frames 2–71 to 84 and 2–17 to 23 dated from 9–19–1937, and frames

3–26 to 37 dated 9–21–1937, black and white, approximate scale 1:20,000.

USDA Agricultural Stabilization and Conservation Service, 1971, Aerial photography, Project AAL, Roll No. 2MM, frames 1–16, 63–77, 82–94, and 139–151 dated 10–9–1971, black and white, approximate scale 1:20,000.

USDA National Agriculture Imagery Program (NAIP), 2009, Digital aerial stereo-photography, image size 12 microns or 2117 pixels per inch, 3-band natural color, approximate scale 1:40,000.

U.S. Natural Resources Conservation Service (NRCS), 2010, Soil survey geographic (SSURGO) database for Salt Lake area, Utah: Online, https://websoilsurvey.sc.egov.usda.gov/App/WebSoilSurvey.aspx, accessed January 30, 2013.

Utah Automated Geographic Reference Center (AGRC), State Geographic Information Database, 2011, 1-meter lidar elevation data: Online, Utah Automated Geographic Reference Center, https://gis.utah.gov/data/elevation-terrain-data/2011-lidar/.

Vanden Berg, M.D., Chidsey, T.C. Jr., Eby, D.E., and Kelln, W., 2015, Characterization of microbialites in Bridger Bay, Antelope Island, Great Salt Lake, Utah [abstract]: Sixth International Limnogeology Congress—abstract volume, Reno, Nevada, June 15–19, U.S. Geological Survey Open-File Report 2015–1092, p. 216–217.

Vanden Berg, M.D., Eby, D.E., Chidsy, T.C., Jr., and Stimpson, R.W., 2016, Characterization of microbialites from Antelope Island's Bridger Bay and Promontory Point, Great Salt Lake, Utah [abstract]: American Association of Petroleum Geologists Annual Convention & Exhibition, June 19–22, Calgary, Alberta, Canada, http://www.searchanddiscovery.com/abstracts/html/2016/90259ace/abstracts/2382481.html.

Van Horn, R., 1979, Surficial geologic map of the Salt Lake City South quadrangle, Salt Lake County, Utah: U.S. Geological Survey Miscellaneous Investigations Series Map I–1173, 1 plate, scale 1:24,000.

Van Horn, R., 1981, Geologic map of pre-Quaternary rocks of the Salt Lake City North quadrangle, Davis and Salt Lake Counties, Utah: U.S. Geological Survey Miscellaneous Investigations Series Map I–1330, 1 plate, scale 1:24,000.

Van Horn, R., 1982, Surficial geologic map of the Salt Lake City North quadrangle, Davis and Salt Lake Counties, Utah: U.S. Geological Survey Miscellaneous Investigations Series Map I–1404, 1 plate, scale 1:24,000.

Viveiros, J.J., 1986, Cenozoic tectonics of the Great Salt Lake from seismic reflection data: Salt Lake City, University of Utah, M.S. thesis, 81 p.

Wallace, J., and Lowe, M., 2009, Ground-water quality classification for the principal basin-fill aquifer, Salt Lake Valley, Salt Lake County, Utah: Utah Geological Survey Open-File Report 560, 80 p., 3 plates, scale 1:75,000.

Williams, S.K., 1994, Late Cenozoic tephrochronology of deep sediment cores from the Bonneville basin, northwest Utah: Geological Society of America Bulletin, v. 105, p. 1517–1530.

Willis, G.C., and Jensen, M.E., 2000, Tertiary rocks of Antelope Island, Davis County, northern Utah, *in* King, J.K., and Willis, G.C., editors, The geology of Antelope Island, Davis County, Utah: Utah Geological Survey Miscellaneous Publication 00–1, p. 49–70.

Willis, G.C., Yonkee, W.A., Doelling, H.H., and Jensen, M.E., 2010, Geology of Antelope Island State Park, Utah, *in* Sprinkel, D.A., Chidsey, T.C., Jr., and Anderson, P.B., editors, Geology of Utah's parks and monuments: Utah Geological Association Publication 28, third edition, p. 349–377.

Wilson, E.A., Saugy, L., and Zimmermann, M.A., 1986, Cenozoic tectonics and sedimentation of the eastern Great Salt Lake area, Utah: Bulletin de la Société Géologique de France, no. 5, p. 777–782.

Yonkee, W.A., 1990, Geometry and mechanics of basement and cover deformation, Farmington Canyon Complex, Wasatch Range, Utah: Salt Lake City, University of Utah, Ph.D. dissertation, 255 p.

Yonkee, W.A., 1992, Basement-cover relations, Sevier orogenic belt, northern Utah: Geological Society of America Bulletin, v. 104, p. 280–302.

Yonkee, W.A., and Lowe, M., 2004, Geologic map of the Ogden 7.5′ quadrangle, Weber and Davis Counties, Utah: Utah Geological Survey Map 200, 42 p., 2 plates, scale 1:24,000.

Yonkee, W.A., Willis, G.C., and Doelling, H.H., 2000a, Petrology and geologic history of the Precambrian Farmington Canyon Complex, Antelope Island, Utah, *in* King, J.K., and Willis, G.C., editors, The geology of Antelope Island, Davis County, Utah: Utah Geological Survey Miscellaneous Publication 00–1, p. 5–36.

Yonkee, W.A., Willis, G.C., and Doelling, H.H., 2000b, Proterozoic and Cambrian sedimentary and low-grade metasedimentary rocks on Antelope Island, *in* King, J.K., and Willis, G.C., editors, The geology of Antelope Island, Davis County, Utah: Utah Geological Survey Miscellaneous Publication 00–1, p. 37–47.

Youngs, R.R., Swan, F.H., Power, M.S., Schwartz, D.P., and Green, R.K., 1987, Probabilistic analysis of earthquake ground shaking hazards along the Wasatch Front, Utah, *in* Gori, P.L., and Hays, W.W., editors, Assessment of regional earthquake hazards and risk along the Wasatch Front, Utah, Volume I: U.S. Geological Survey Open-File Report 87-585, p. M-1–110.

Zoback, M.L., 1983, Structure and Cenozoic tectonism along the Wasatch fault zone, Utah, *in* Miller, D.M., Todd, V.R., and Howard, K.A., editors, Tectonic and stratigraphic studies in the eastern Great Basin: Geological Society of America Memoir 157, p. 3–27.